PHYSICAL REVIEW B VOLUME 18, NUMBER 10 15 NOVEMBER, 1978

First-principles nonlocal-pseudopotential approach in the density-functional formalism: Development and application to atoms

Alex Zunger and Marvin L. Cohen
Department of Physics, University of California and Materials and Molecular Research Division, Lawrence Berkeley Laboratory, Berkeley, California 94720
(Received 22 May 1978)

We present a method for obtaining first-principles nonlocal atomic pseudopotentials in the density-functional formalism by direct inversion of the pseudopotential eigenvalue problem, where the pseudo-wave-functions are represented as a unitary rotation of the "exact" all-electron wave functions. The usual pseudopotential nonuniqueness of the orbitals is fixed by imposing the physically appealing constraints of maximum similarity to the all-electron wave functions and minimum radial kinetic energy. These potentials are shown to yield very accurate energy eigenvalues, total energy differences, and wave-function moments over a wide range of excited atomic configurations. We have calculated the potentials for 68 transition and nontransition elements of rows 1–5 in the Periodic Table. Their characteristic features, such as classical turning points and minimum potential radii, faithfully reflect the chemical regularities of the Periodic Table. The nonempirical nature of these potentials permits both an analysis of their dominant features in terms of the underlying interelectronic potentials and the systematic improvement of their predictions through inclusion of appropriate correlation terms. As these potentials accurately reproduce both energy eigenvalues and wave functions and can be readily fit to analytic forms with known asymptotic behavior, they can be used directly for studies of many structural and electronic properties of solids (presented in a separate paper).

I. INTRODUCTION

Pseudopotentials have enjoyed enormous popularity in the past decade in a very wide range of problems, including electronic structure of atoms,[1] molecules,[2] solids,[3,4] surfaces[5] and interfaces,[6] structural stability of crystal phases,[4,7] phonon dynamics,[8] transport properties,[9] and superconductivity.[10] The basic underlying notion has been that the closed-shell core states, with their approximate spherical symmetry and tight-binding character, are nearly unresponsive to many of the low-energy perturbations that are responsible for the physically interesting phenomena in the subspace of the "reactive," or valence states. As a matter of fact, the entire notion of the column structure of the Periodic Table is based on this passivity of the core states to variations in the bonding environment. Since a large number of quantum-mechanical approaches to the many-electron problem involve mathematical operations whose complexity increases as a high power of the total number of electrons in the unit system, an explicit reckoning of the core electrons has become redundant.

Despite these difficulties, the vast majority of *ab initio* studies of molecular and solid-state electronic structure has been based in the past on a frontal attack on the all-electron (core + valence) problem, most notably within the Hartree-Fock and local-density-functional (LDF) formalisms. Although the introduction of various simplifying approximations to the all-electron potential (e.g., muffin-tin approximations, limited self-consistency, superposition approximations, etc.) has enabled the study of rather complex molecular and solid-state systems, even with the aid of modern computing technology, more rigorous approaches are still limited to the study of small to medium size systems. Aside from the practical difficulties with the all-electron approach, more fundamental complications arise from the necessity to establish orthogonality to the *exact* lower states of the Hamiltonian in order to assure the variationality of the expectation values,[11] and the lack of transferability of the elementary constructs of the electronic structure (e.g., core characteristics) from one system to the other, a universality that underlines much of the intuition of chemical bonding.

The most obvious approach has been to explicitly ignore the core electrons. Since unrestricted variational solutions to the problem would inevitably result in an attempt of the valence states to reproduce the lowest-energy corelike states[12] ("variational collapse" to the core), an explicit parametrization of the valence Hamiltonian (or its matrix elements) has been required. This approach formed the basis for a large number of semiempirical electronic-structure methods, both in chemistry [Hückel,[13] Pariser-Parr-Pople (PPP),[14] CNDO[15]] and in solid-state physics (classical tight binding,[16] Hubbard,[17] Kondo,[18] etc.). The pseudopotential approach[19-21] has allowed one to formally

substitute the all-electron problem:

$$(-\tfrac{1}{2}\nabla^2 + V_{v,c})\psi_j = \epsilon_j \psi_j \tag{1}$$

[where ψ_j spans the combined core (c) and valence (v) orthogonal subspaces, and $V_{v,c}$ is determined in principle from all ψ_j's], with a simpler equation

$$(-\tfrac{1}{2}\nabla^2 + V_v + V_{\mathrm{PS}})\chi_i = \lambda_i \chi_i , \tag{2}$$

where i spans only the valence subspace and the χ_i's are related to the ψ_j's by a unitary rotation

$$\chi_i = \sum_{j'} C_{ij'} \psi_{j'} \tag{3}$$

with arbitrary constant coefficients $C_{ij'}$. Here V_v has the same functional form as $V_{v,c}$, but acts only on the valence subspace, while V_{PS} is an additional potential (hereafter denoted the pseudopotential), determined in principle from the spectrum ϵ_j, vector space $\{\psi_j\}$, and transformation coefficients $\{C_{ij}\}$, such that $\lambda_i = \epsilon_i$ for all valence states. Transformation (3) makes it possible (but not necessary) to obtain smooth and nodeless orbitals χ_i, simply by mixing sufficient core states ψ_j^c into the valence state ψ_j^v, to remove its spatial nodes. Consequently, the set $\{\chi_i\}$ does not have to be orthogonal to the core. To the extent that the construction of V_{PS} can be made sufficiently simple, the pseudopotential eigenvalue problem (2) is substantially easier to handle than the original problem (1). The fact that the pseudo-wave-functions (3) are just a linear combination of the all-electron states makes it possible to recover the true wave functions ψ_j from the solutions χ_i simply by orthogonalizing to the (usually known) core states.[20,22] Phillips and Kleinman[20] have shown that for the particular case where the core functions ψ_j^c are eigenstates of the Hamiltonian describing the valence manifold, the pseudopotential V_{PS} can be written in the relatively simple form

$$V_{\mathrm{PS}}(r, \epsilon^v) = \sum_{j \in c} (\epsilon^v - \epsilon_j^c) \left| \psi_j^c \right\rangle \left\langle \psi_j^c \right| . \tag{4}$$

Unfortunately, the above condition simply does not hold for most systems of interest (e.g., for single-valence-electron atoms or ions, the core orbitals are eigenstates of a Hartree-Fock Hamiltonian that includes both core and valence terms[23]). A generalization of Eq. (4) to many-valence-electron systems by Weeks and Rice[12] results in a very complicated form for V_{PS} in terms of the core-projected valence wave functions, core orbitals, and pseudo-wave-functions, and hence does not lead to any simplification of Eq. (1). Even the simpler form (4) requires the knowledge of the actual solutions of the all-electron problem of the system of interest, and hence is of little direct help. The inherent simplification provided by the pseudopotential approach in replacing the all-electron potential and the orthogonal set ψ_j by an *effective* potential,

$$V_{\mathrm{eff}} = V_{\mathrm{PS}} + V_v , \tag{5}$$

with its associated non-core-orthogonal set, rests in the possibility to construct V_{PS} from the core characteristics of some simple *prototype* system and to use this potential for studying the response of the reactive electrons in *general* systems. This constitutes the basic *pseudopotential frozen-core approximation*, which replaces the dynamic effects of the core electrons in an arbitrary system by a static external field constructed from the core characteristics of simpler reference systems. Such a potential is considered successful if that replacement holds over a sufficiently large energy range (e.g., a typical width of a valence and lower conduction bands). The potential is then said to be approximately energy independent over that range.

These ideas have led to two distinct approaches in implementing the pseudopotential theory in practice—the model potential and the first-principles potential methods. The model potential approach abandons the relation (3) between the pseudo- and real wave-functions, and usually uses an ansatz functional form for either V_{PS} or $V_{\mathrm{PS}} + V_v$ (to be fixed by fitting to some selected properties of prototype systems) such that the energy eigenvalues of the new potential match those of the real potential over some energy range. One hence gives up the control one had on the *wave functions* [(e.g., by fixing the C_{ij} in Eq. (3))], and concentrates on reproducing the *energy eigenvalue spectra*. This approach was originally stimulated by the apparent difficulties reported in the mid-1960's by Abarenkov and Heine[24] and Szasz and McGinn[25] to obtain directly from Eq. (4) simultaneously smooth pseudopotentials and wave functions, even for simple ions. The model potential approach has been subsequently used in three major forms: the empirical-pseudopotential method (EPM), the semiempirical self-consistent pseudopotential method (SSPM), and the nonempirical-model-potential method (NEMP). In the EPM approach[3,26,27] one completely avoids the specification of the microscopic interactions pertaining to V_v (e.g., Coulomb, exchange, and correlation) and obtains a parametrized V_{eff} directly by fitting the energy eigenvalues of Eq. (2) to low-energy spectra of semiconductors,[3,26,27] for Fermi-surface data,[28] or ionic term values.[29,30] The translational symmetry of the perfect solid and the relative insensitivity of the electronic structure near the Fermi energy to high-momentum-transfer scattering events, made it possible to obtain a good fit using

only a small number of parameters $V_{eff}(\vec{G}_i)$, where $\vec{G}_i$ is a reciprocal-lattice vector. Systematic extension of this approach is possible via the introduction of additional parametric forms in V_{eff}, describing the energy and angular momentum dependence of the pseudopotential[27] (nonlocal corrections). As the separation of the potential indicated in Eq. (5) is not done in the EPM, this approach is not limited by the frozen-core approximation and attempts to mimic core polarization and relaxation effects. The SSPM approach[31-33] treats the valence field by a microscopically defined theory [e.g., Hartree-Fock[33] (HF) or local-density functional (LDF)[32]], but parametrizes a chosen model form for V_{PS} to ionic term values[32] or to the band structure.[31] Since in this approach V_{eff} depends on the actual solutions χ_i through the screening valence field $V_v(\sum_i \chi_i^2)$, self-consistency in the description is possible in principle. In the NEMP approach,[34-37] V_v is again treated rigorously while V_{PS} is fitted to theoretically calculated all-electron atomic eigenvalues.

In contrast to all the model potential approaches, the first-principles pseudopotential approach retains the rigorous relation (3) and attempts to calculate both V_{PS} and V_v from a microscopic theory without restricting them to any model functional form. Both the successes and the failures of this theory in reproducing the observed data can in principle be analyzed in terms of the underlying microscopic interactions in the Hamiltonian (e.g., electron correlation), subject to the pseudopotential frozen-core approximation. Further, property (3) enables the retention of the desirable features in the pseudo-wave-functions (such as expandability in simple and convenient basis functions, similarity to "good" all-electron wave functions, etc.) and recovery, to within a good approximation, of the true wave functions, simply by core orthogonalization.

First-principles pseudopotentials have been previously obtained with the HF scheme by several workers,[1,23,38,39] and were used for molecular structure studies. Recently, Zunger *et al.*[40,41] have suggested a method for obtaining first-principles pseudopotentials in the local-density formalism which are more directly suitable for solid-state applications. In this paper we present a generalization of the method to all atoms of rows 1–5 in the Periodic Table. This enables a comprehensive discussion of the chemical regularities in these potentials, including the variations in their nonlocality, strength, and characteristic turning points as a function of their location in the Periodic Table. We show that these potentials very accurately reproduce both the wave functions and the energy eigenvalues and total energy differences of the underlying all-electron density-functional Hamiltonian over a wide range of excited states. This establishes their weak energy dependence over a large range of electronic configurations and orbital delocalization, and suggests their usefulness for studying bonded atoms in solids. We further demonstrate how the agreement obtained with observed quantities can be systematically improved by introducing appropriate correlation corrections into the all-electron Hamiltonian. In a separate paper we will discuss applications to both bulk-solid electronic structure and to the study of the phase stability of crystal structures. Their success in describing both electronic properties and structural regularities will hopefully enable the establishment of the pseudopotential practice in solid-state theory on a basis of a microscopic first-principles theory.

II. DEVELOPMENT OF THE FIRST-PRINCIPLES PSEUDOPOTENTIALS

As the underlying ideas of the development of the first-principles pseudopotential in the local-density formalism have been presented previously,[40,41] we give here only a brief discussion and indicate the new features needed to treat atoms in arbitrary position in the Periodic Table.

One considers a fictitious (pseudo) atom in a reference electronic state g, having N_v electrons (where N_v is the number of electrons in the true atom assigned to valence states) and a nuclear charge Z_v. The electrons interact via Coulomb and exchange-correlation forces and with a (yet unspecified) fixed external potential given by

$$V_{ext}(r) = -Z_v/r + V_{PS}(r) . \tag{6}$$

The total energy of the system is

$$E_t^g[n] = T_0(n_g) + \int n_g(r) V_{ext}(r)\, dr + \frac{1}{2}\int \frac{n_g(r) n_g(r')}{|r-r'|}\, dr\, dr' + E_{xc}(n_g) , \tag{7}$$

where $T_0(n_g)$ is the noninteracting kinetic energy of electron density n_g and $E_{xc}(n_g(r))$ is the interacting, inhomogeneous total exchange and correlation energy.[42] One expects that the effective one-particle equation that will determine the variational density in Eq. (7) will be[42,43]

$$[-\tfrac{1}{2}\nabla^2 + V_{ext}(r) + V_{ee}(n_g(r)) + V_{xc}(n_g(r))]\chi_{nl}^g(r) = \lambda_{nl}^g \chi_{nl}^g(r), \tag{8}$$

where the interelectronic Coulomb and exchange-

correlation potentials are, respectively,

$$V_{ee}(n_g(r)) = \int \frac{n_g(r')}{|r-r'|}\,dr',$$

$$V_{xc}(n_g(r)) = \frac{\delta E_{xc}(n_g(r))}{\delta n_g(r)}, \tag{9}$$

and the density $n_g(r)$ is related self-consistently to the eigenvectors of Eq. (8) by

$$n_g(r) = \sum_{nl} N^g_{nl} |\chi^g_{nl}(r)|^2. \tag{10}$$

Here N^g_{nl} denotes the valence occupation number in the ground reference state g, and the sum is extended to include N_v electrons. The inhomogeneous exchange and correlation potential $V_{xc}(n_g(r))$ is normally replaced by the homogeneous free-electron potential $V_{xc}(n_g(r))$ in the usual way,[42] leading to an exchange part $V_x(n_g(r))$ [with exchange coefficient $\alpha = \frac{2}{3}$ (Ref. 42)] and a correlation part $V_c(n_g(r))$ for which we adopt the results of Singwi *et al.*[44] Gradient corrections[42,45] are possible, but will not concern us here. Note that as the density $n_g(r)$ would be constructed to be slowly varying over space, the neglect of the higher terms in the gradient expansion is more justified than in the all-electron LDF approach.

One now seeks the form of the external potential $V_{ext}(r)$ such that for the reference electronic state g, the eigenvalues of Eq. (8) will equal those of the *all-electron* problem:

$$[-\tfrac{1}{2}\nabla^2 - (Z_v + Z_c)/r + V_{ee}(\rho_g(r)) + V_{xc}(\rho_g(r))]\psi^g_{nl}(r) = \epsilon^g_{nl}\psi^g_{nl}(r), \tag{11}$$

and that the pseudo-orbitals $\chi^g_{nl}(r)$ will be related to the all-electron solutions $\psi^g_{nl}(r)$ by a simple unitary rotation

$$\chi^g_{nl}(r) = \sum_{n'}^{M} C^g_{nl,n'l}\psi^g_{n'l}(r), \tag{12}$$

where $\{C^g_{nl,n'l}\}$ are arbitrary coefficients, to be fixed later. We denote the all-electron and pseudo-charge-densities by $\rho(r)$ and $n(r)$, respectively, and add the indices v and c to denote valence and core, when necessary. This condition determines the external potential in terms of the (reference state) all-electron quantities and the transformation $\{C^g_{nl,n'l}\}$ as

$$V_{PS}(r) = \epsilon^g_{nl} + \frac{1}{2}\frac{\nabla^2\chi^g_{nl}(r)}{\chi^g_{nl}(r)} - \left[-Z_v/r + V_{ee}(n_g(r)) + V_{xc}(n_g(r))\right]. \tag{13}$$

Here we have used the fact that $V_{xc}(n_g(r))$ is a local function (if gradient terms are to be included, an appropriate average over the orbitals $\psi^g_{nl}(r)$ is taken[41]). Expressing the second term in Eq. (13) by the all-electron form (11), one obtains

$$V_{PS}(r) = U_l(r) + V_{tot}(\rho_g(r)) - V_v(n_g(r)), \tag{14}$$

where $U_l(r)$ is

$$U_l(r) = \frac{\sum_{n'} C^g_{nl,n'l}(\epsilon^g_{nl} - \epsilon^g_{n'l})\psi^g_{n'l}(r)}{\sum_{n'} C^g_{nl,n'l}\psi^g_{n'l}(r)} \tag{15}$$

and $V_{tot}(\rho_g(r))$ is the total all-electron potential of Eq. (11). The sums in Eq. (15) are over all core states and the nlth valence state, and $V_v(n_g(r))$ is the valence field due to the distribution $n_g(r)$ and the nuclear charge Z_v [last term in square brackets in Eq. (13)].

In this form, $V_{PS}(r)$ can be used in Eq. (8) to replace the core electrons of Eq. (11) and produce the desired eigenvalue spectra and wave functions. It is, however, directly expressed in terms of the all-electron solution and, as such, is of little help. We assume now the pseudopotential frozen-core approximation, namely, that $V_{PS}(r)$, which exactly replaces the dynamic effects of the core electrons *in the reference atomic electronic state* g, can be used for states other than g. This implies that if $V_{PS}(r)$ is obtained for a characteristic state g from Eq. (14), then one can directly obtain approximate valence-electron solutions for arbitrary systems containing the same core through the use of the pseudopotential rather than the all-electron equation. A large part of the rest of this paper is devoted to testing and discussing this approximation.

We now examine how the freedom given in transformation (12) can be used to obtain useful results. In order for the pseudopotential to correctly reproduce the chemical content of the underlying all-electron problem, one would like $\chi_{nl}(r)$ to be as close as possible to the true orbital $\psi^v_{nl}(r)$ in the regions of space which are relevant for bonding in polyatomic systems. One would similarly require that $\chi_{nl}(r)$ be spatially smooth and lack the radial nodes characteristic of $\psi_{nl}(r)$ [as $\chi_{nl}(r)$ are now the *lowest* solution of the new Hamiltonian in Eq. (2)], so that the former be conveniently expandable in simple and small basis sets. This would permit direct comparison of the valence orbitals of atoms belonging to the same row without reference being made to their differences in the chemically passive core regions. Whereas the smoothness of the pseudo-wave-functions can be imposed by mixing sufficient core orbitals in transformation (12), undue "overmixing" can result in lack of similarity of $\chi_{nl}(r)$ to the corresponding all-electron valence orbitals in the chemically important tail region. A straightforward method that fulfills this "maximum similarity" constraint within a nonor-

thogonal representation is the simultaneous minimization of the core-projection expectation value

$$\langle \chi_{nl}(r) | \hat{P}_c | \chi_{nl}(r) \rangle = \min \tag{16}$$

for all valence states nl, subject to the requirement that $\chi_{nl}(r)$ be nodeless.[23,41] A simple illustration of this process can be given for first-row atoms: here one finds that the *minimum* amount of mixing of the core $\psi_{1s}(r)$ orbital into the valence $\psi_{2s}(r)$ orbital, which produces a normalized and nodeless $\chi_{2s}(r)$ orbital, leads to $\chi_{2s}(0)=0$. Any further mixing of $\psi_{1s}(r)$ would still yield a nodeless $\chi_{2s}(r)$, however, its similarity to $\psi_{2s}(r)$ would diminish. Minimization of the core projection within the constraint of $\chi_{2s}(r)$ being nodeless is hence simply equivalent here to requiring $\chi_{2s}(0) = C_{1s,2s}\psi_{2s}(0) + C_{2s,2s}\psi_{2s}(0) = 0$. Clearly, condition (16) uniquely determines the pseudopotential transformation for the simple case of a single core orbital. For atoms having an arbitrary number of core states, we follow the suggestion of Kahn *et al.*[23] and require that the optimum pseudo-orbital also minimize the "radial kinetic energy",

$$\int_0^\infty \left[\frac{d}{dr}\left(\frac{\chi_{nl}(r)}{r_l}\right)\right]^2 dr = \min, \tag{17}$$

and hence be spatially smooth. Conditions (16) and (17), subject to the additional requirement of normalization and least amplitude in the inner-core region $\chi_{nl}(0)=0$ (equivalent to the cusp condition[23]), uniquely determine transformation (12). Some examples for the optimum coefficients are given in Appendix A.

The crucial step here is that we do not allow the process of fitting the energy eigenvalues of the pseudo-Hamiltonian to some selected canonical results to also implicitly fix the pseudo-wave-functions to some uncontrolled form.[3,26,27] We similarly avoid the use of core-projection operators directly in the pseudopotential, as done in the Phillips-Kleinman form,[20] simply because such a choice leads to arbitrary wave functions in an unconstraint variational treatment. Instead, we fix the nonuniqueness of the pseudo-wave-functions in the reference electronic state from the outset by imposing the physically appealing constraints of maximum wave-functions similarity and minimum kinetic energy. Any successful constraint of this sort should result in pseudo-wave-functions that systematically reproduce the characteristics of the true wave functions in a reasonably wide energy range. We examine this question quantitatively in Sec. IV.

The numerical procedure used to solve Eqs. (8) and (11) were previously discussed.[40] It consists of a self-consistent predictor-corrector numerical integration scheme that avoids the need of expanding $\psi(r)$ in basis sets and produces very accurate ($\sim 10^{-7}$ a.u. in the energies) and stable results. The determination of the pseudo-orbitals in Eq. (12) is performed iteratively by progressively mixing core orbitals with valence orbitals and minimizing Eqs. (16) and (17) simultaneously. The required transformation coefficients $C_{nl,n'l}$ are obtained as the lowest roots of a $M \times M$ eigenvalue problem pertaining to the matrix form of Eqs. (16) and (17). Accurate solutions of Eq. (17) require the knowledge of the polynomial expansion of $\psi_{nl}(r)$ at small r.[46] The first three to four terms in such an expansion are sufficient to determine $C_{nl,n'l}$ to six significant figures. These calculations have been performed for 68 atoms from rows 1–5 in the Periodic Table. The resulting pseudopotentials and their quality are discussed in the next few sections.

III. FORM OF THE CORE POTENTIALS AND CHEMICAL TRENDS

Figures 1–5 depict the form of some representative nonlocal atomic core potentials. The atomic core potential $W_l(r)$ is defined by combining the nuclear attraction term $-Z_v/r$ from the valence po-

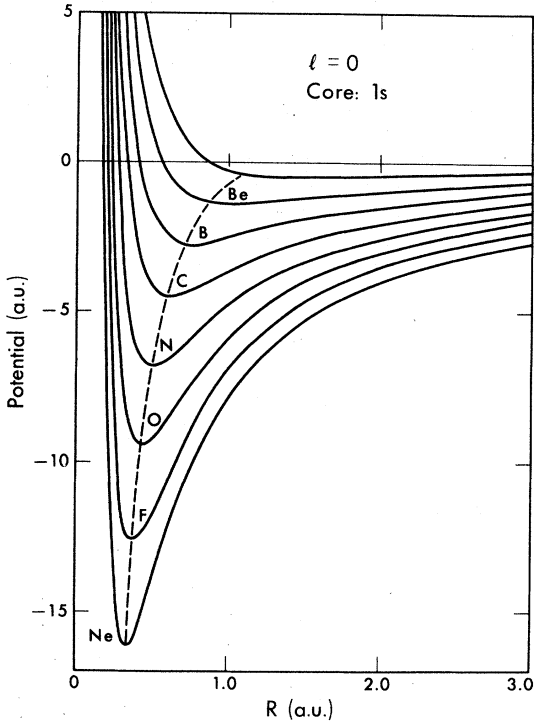

FIG. 1. The $l=0$ core potentials of the first-row atoms. Due to the absence of $l=1,2$ core states in these systems, the core potentials of the latter symmetries (not shown) are purely attractive.

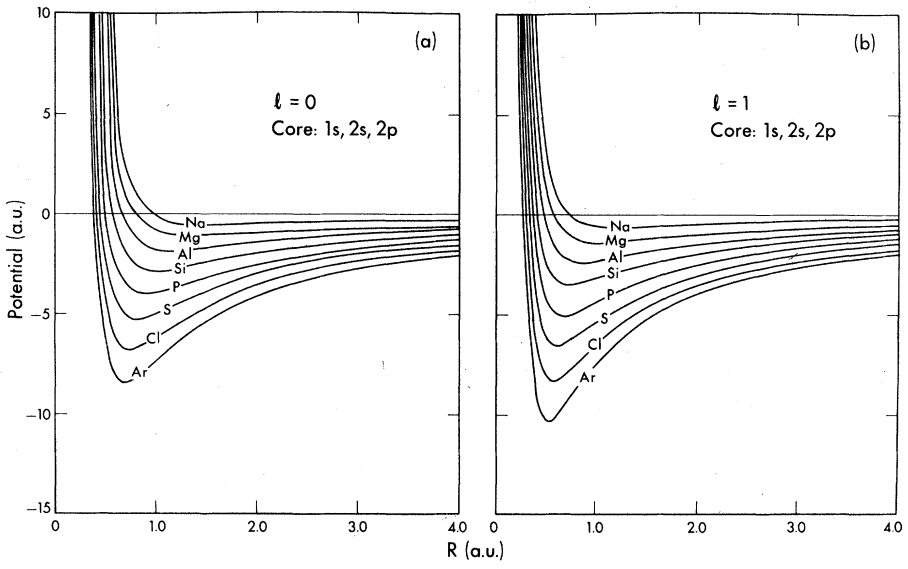

FIG. 2. Core potentials of second-row atoms. (a) $l=0$, (b) $l=1$. The $l\geq 2$ potentials are purely attractive.

tential in Eq. (5) with the pseudopotential

$$W_l(r) = V_{\rm PS}^{(l)}(r) - Z_v/r \tag{18}$$

(This term is usually referred to in the literature as "ionic potentials". We prefer to use here the atomic core potential to indicate that $W_l(r)$ replaces an *atomic* core rather than the core of a stripped *ion*). The term $Z_v^* = -rW_l(r) + Z_v$ can be viewed as a position and angular-momentum-dependent effective charge that replaces, in the pseudopotential representation, the actual valence charge Z_v. In generating these core potentials for atoms from the ith row in the Periodic Table, we have defined the core orbitals as those belonging to the rare-gas atom from row $i-1$.

In order to understand the form of the atomic core potentials in Figs. 1–5, we first rewrite $W_l(r)$ in terms of the components of the all-electron potential and the all-electron and pseudo-charge-densities $\rho(r)$ and $n(r)$, respectively. Using Eq. (14) and adding and subtracting $V_{xc}(\rho^v(r))$ $+ V_{xc}(\rho^c(r))$, one gets

$$\begin{aligned} W_l(r) = &[U_l(r) - Z_v/r] \\ &+ [-Z_c/r + V_{ee}(\rho^c(r)) + V_{xc}(\rho^c(r))] \\ &+ [V_{xc}(\rho^c(r) + \rho^v(r)) \\ &\quad - V_{xc}(\rho^c(r)) - V_{xc}(\rho^v(r))] \\ &+ [V_{ee}(\rho^v(r)) - V_{ee}(n^v(r))] \\ &+ [V_{xc}(\rho^v(r)) - V_{xc}(n^v(r))], \end{aligned} \tag{19}$$

where $U_l(r)$ is given by Eq. (15). Here the first term represents the nonlocal, or l-dependent part, while the rest of the terms are "local" (i.e., common to all l values). In applying these core potentials to polyatomic systems, $W_l(r)$ is considered as an external potential associated with a given core and the *total* core potential is given by

$$W_{\rm tot}(\vec{\mathbf{r}}) = \sum_\alpha \sum_l W_l(\vec{\mathbf{r}} - \vec{\mathbf{R}}_\alpha)\hat{P}_{l\alpha}\,, \tag{20}$$

where $\vec{\mathbf{R}}_\alpha$ denotes the position vector of the αth core, and $\hat{P}_{l\alpha}$ is the angular momentum projection operator with origin at $\vec{\mathbf{R}}_\alpha$.

The atomic core potential in Eq. (19) has a simple physical interpretation. The term $U_l(r)$ replaces the core-valence orthogonality constraint for those pseudo-orbitals that have lost spatial nodes due to transformation (12). The valence orbitals that have no core states of matching symmetry (e.g., $2p$, $3d$ for first-row atoms, $3d$ for second-row and the first-transition-series atoms, etc.) are already nodeless in the all-electron orthogonal representation, and no core mixing via Eq. (12) is needed; in these cases $\chi_{nl}(r) \equiv \psi_{nl}(r)$ represents the nodeless maximum-similarity orbital, and the sum in Eq. (15) reduces to a single term as $C_{nl,n'l} = \delta_{n,n'}$. Hence $U_L(r) \equiv 0$ for all $l = L$ not present in the core. We see that for these l values the atomic core potential is local and common to all $l = L$. The effective potential (5) seen by such an electron in the atom is simply the total all-electron potential $V_{\rm tot}(\rho(r))$ with $\lim_{r\to 0} W_l(r) = -Z/r$, and no pseudopotential cancellation is said to take place. On the other hand, valence orbitals that have core states of matching symmetry are mixed with the latter in transformation (12). This leads to a strongly repulsive $U_l(r)$ in Eq. (15). In particular, if $\chi_{nl}(r)$ in Eq. (12) is chosen to have zero amplitude at the origin, a polynomial expansion of $\psi_{nl}(r)$ leads to[23,41]

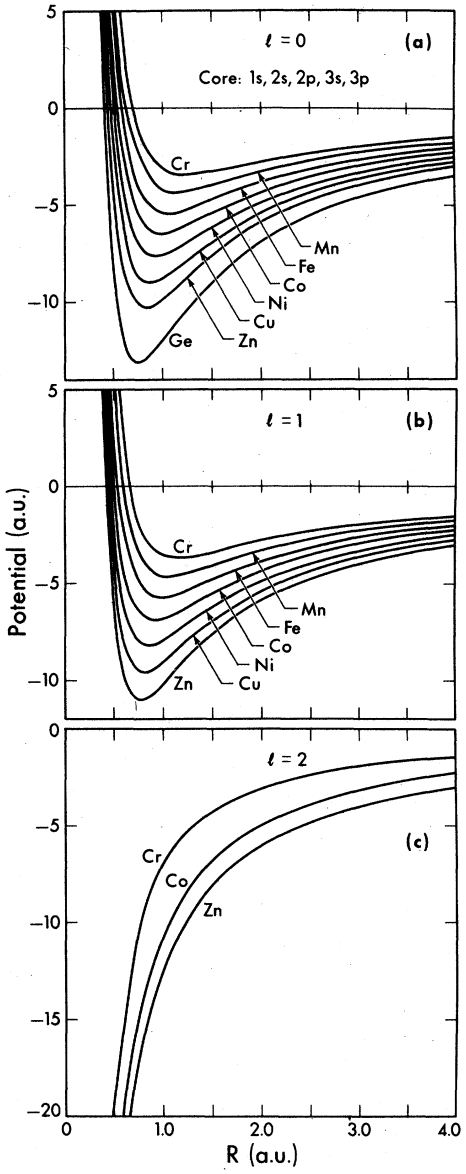

FIG. 3. Core potentials of the first, $3d$, transition series (a) $l=0$, (b) $l=1$, and (c) $l=1$.

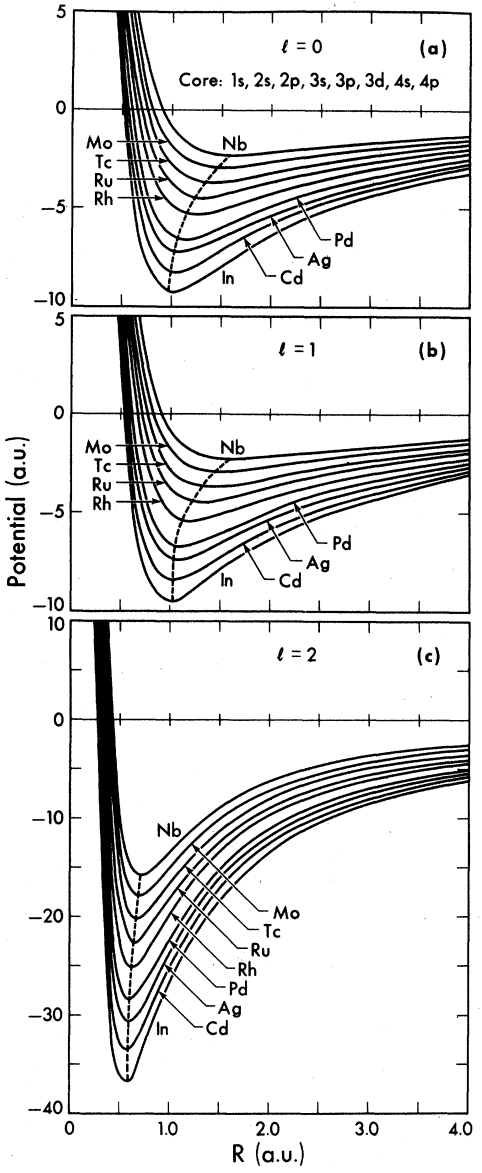

FIG. 4. Core potentials of the $4d$ transition series (a) $l=0$, (b) $l=1$, and (c) $l=2$.

$$\lim_{r\to 0} U_l(r) = C_l/r^2 \qquad (21)$$

for $l \neq L$ where C_l is a positive constant. It is hence seen that $U_l(r)$ replaces an effective centrifugal barrier for those states that have been "pseudized" by transformation (12). $U_l(r)$ is hence a realization of Pauli's exclusion principle as a potential in real space, and is responsible for the "hard-core" behavior of the core potentials in Figs. 1–5 for $l \neq L$. This repulsive potential tends to partially cancel the nuclear attraction term in Eq. (19), leading to a form that is "weaker" (i.e., has valence rather than core states as the lowest solutions) than the all-electron potential. Note that in the present formulation the degree of this pseudopotential cancellation is not assumed (viz., the empty-core[28] or Heine-Abarenkov[24] potentials), but rather comes out as a natural consequence of the maximum similarity constraint imposed on the orbital transformation in Eq. (12). Had we, for instance, given up the requirement that the pseudo-wave-function match the true wave function to the maximum degree possible for a nodeless orbital χ, the pseudopotential cancellation in Eq. (19) would have been altered significantly. An extreme illustration is the case where the pseudo-orbital

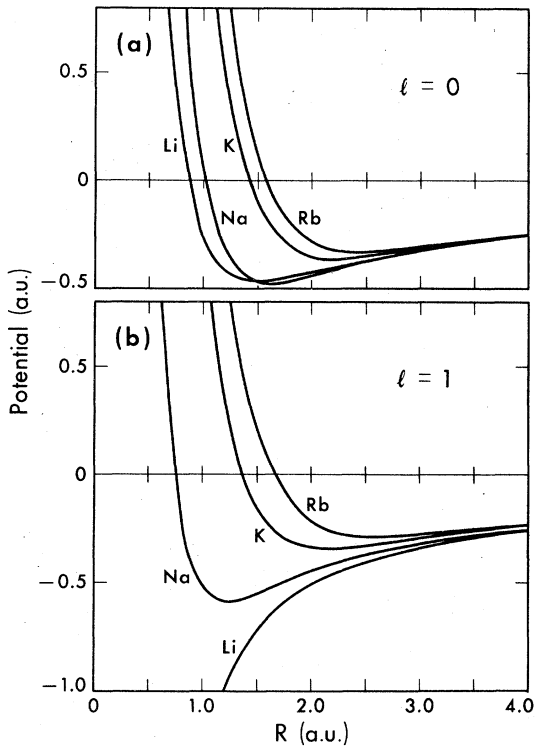

FIG. 5. Core potentials of the alkali atoms. (a) $l=0$, (b) $l=1$.

$\chi_{nl}(r)$ is identified in Eq. (12) with a $1s$ orbital [having no nodes but lacking similarity to the valence state $\chi_{nl}(r)$]. This leads to $U_l(r)=\epsilon_{nl}-\epsilon_{1s}$, exactly like the Phillips-Kleinman form,[20] with little pseudopotential cancellation. Clearly, this resulting core potential would yield the correct valence *eigenvalues* in Eq. (2) (simply by shifting the $1s$ level by an amount necessary to make it degenerate with the valence orbital of interest), but would lead to very poor valence *wave functions*. The highly repulsive character of $U_l(r)$, $l\neq L$, for small r and the associated degree of pseudopotential cancellation is hence a natural consequence of the maximum similarity constraint on the pseudo-wave-functions, which assures in turn its variational quality. Note that the repulsive nonlocal potential $U_l(r)$ is short range under the maximum similarity constraint; if R_c denotes a distance from the origin at which all core orbitals have already decayed to zero, it is clear from Eq. (15) that for $r>R_c$ one gets $U_l(r)=0$. Hence, although determining the behavior of the pseudo-wave-functions in their tail region, $U_l(r)$ is confined to the core region. We note that both the empirical and the semiempirical core potentials used for solid-state applications usually lack this hard-core repulsive behavior near the origin,[3,5,24,26,27,31,32] as the fitting of the pseudopotential energy eigenvalues alone to the low-energy spectra leaves one with the liberty to employ smooth potentials. This is a consequence of the relative insensitivity of the valence electronic structure near the Fermi energy to high-momentum-transfer scattering events. Imposing explicit constraints on the wave functions of the sort discussed above leads to the repulsive core with its characteristic high-momentum components. This is in turn responsible for the formation of the classical turning points satisfying $W_l(r_l^0)=0$, which contain a great deal of structural information and can be used to theoretically separate various crystalline phases.[47,48]

The second term in square brackets in Eq. (19) represents the total Coulomb and exchange-correlation potential of an isolated neutral core. It behaves as $-Z_c/r$ at short distances, and is screened out by the core density further out. The third term in square brackets in Eq. (19) represents the nonlinearity of the exchange-correlation functional with respect to the core and valence charge densities. It measures the core-valence interaction in the system, and is hence proportional to the penetrability of the core by valence electrons (which is a consequence of their mutual orthogonality). The last two terms in square brackets in Eq. (19) ΔV_{ee} and ΔV_{xc} represent, respectively, the Coulomb and exchange-correlation orthogonality hole potentials. They stem directly from the existence of a depletion charge density $\Delta(r)=\rho^v(r)-n(r)$ due to the removal of the orthogonality nodes in the pseudopotential representation. Under the maximum similarity constraint, $\Delta(r)$ is positive in the inner core and becomes negative further out. This leads to a partial cancellation between the electron repulsion $\Delta V_{ee}(r)$ and the exchange-correlation attraction $\Delta V_{xc}(r)$ over the core region. The large r behavior of the atomic core potentials is hence determined by $-Z_v/r$ (or in Fourier space, by $-4\pi e^2 Z_v/q^2$), slightly modified by the sum $\Delta V_{ee}+\Delta V_{xc}$ of the orthogonality hole potentials. These deviate from zero outside the core only to the extent that the pseudo-charge-density $n(r)$ does not exactly mimic the true valence density $\rho^v(r)$. These deviations are in turn explicitly minimized by the maximum similarity constraint[40,41] imposed here. Note that while the all-electron local-density potential $V_{\rm tot}(r)$ (Eq. 11) has an unphysical exponential decay at large r (due to the noncancellation of the Coulomb and exchange self-interactions[43]), the corresponding core potentials lack this feature.

It is clear from our discussion of the atomic core potentials $W_l(r)$ that they are divided into two principle classes: for l not present in the core, they are governed by the $-Z/r$ form at small r and are negative throughout all space, approaching

zero as Z_v/r [e.g., Fig. 3(c)]. For l present in the core, they start out as C_l/r^2 in the inner core, have an l-dependent classical turning point r_l^0 [$W_l(r_l^0)=0$] and a negative minimum $W_l^{\min}=W_l(r_l^{\min})$ at $r_l^{\min}$, and then approach zero as $-Z_v/r$ [e.g., Figs. 3(a), 3(b) and 4]. Their essential new feature relative to many of the empirical model potentials is the occurrence of the turning points[49] r_l^0. These are strongly nonlocal and characterize the properties of the atomic core in that they represent the point where the repulsive Pauli potential, modified by orthogonality hole effects, equals the attractive electron-nuclear and exchange-correlation potentials. Their occurrence in the inner-core region suggests the possibility of their transferability from one system to the other, and makes them particularly suitable for discussing chemical regularities in molecules and solids. Implicit in their derivation are the classical constructs used to describe bonding, such as electronegativities, hybridization, and s-p promotion energies, as r_l^{-1} measures the scattering power of a screened core towards states with angular momentum l. In a separate paper[50] we show that, in fact, these turning points can be used to provide an essentially exact topological separation of the various structural phases of both octet A^NB^{8-N} and the suboctet A^NB^{P-N}, $3 \leq P \leq 6$ compounds.

Figures 1–5 show that systematical changes occur in r_l^0, $r_l^{\min}$, and $W_l^{\min}$ as one moves along rows and columns in the Periodic Table. A better visualization of these trends is provided in Fig. 6, where the elements are denoted by their $(r_l^{\min}, W_l^{\min})$ coordinates. In this plot we have again used a closed-shell rare-gas core for separating the valence states from the core. The elements are seen to be clearly grouped according to their rows in the Periodic Table. At small $|W_l^{\min}|$ and large $r_l^{\min}$ (i.e., shallow and delocalized, or weak, potentials) we find the classical free-electron-like metals, while at large $|W_l^{\min}|$ and small $r_l^{\min}$ (deep and localized, or strong, potentials) we find the atoms that form covalent structures and the transition metals. Each row in the Periodic Table is represented here by at least two lines—one connecting the full circles passing through the $l=0$ coordinates and one connecting open circles passing through the $l=1$ coordinates. The full triangles denote the $l=2$ coordinates. The $l=1$ components of the first-row atoms as well as the $l=2$ components of the second and third rows are purely attractive, as discussed above, and all have a minimum of negative infinity at the origin. For convenience, we have connected the $l=0$ and $l=1$ coordinate of each atom by a straight line. Clearly, the length and slope of these lines measure the s-p nonlocality of the potential. Few interesting observations can be made. The s-p nonlocality decreases as one moves down the columns in the Periodic Table, as the ratio of the number of core

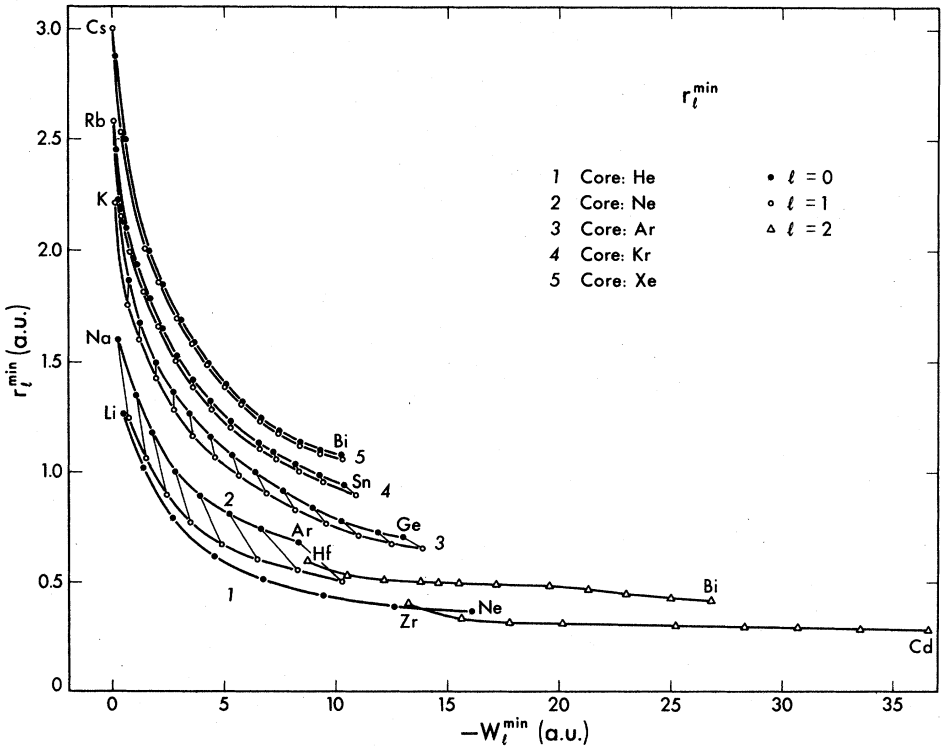

FIG. 6. Radii of minimum potential $r_l^{\min}$ as a function of the well depth $|W_l^{\min}|$ for atoms of rows 1–5. Full circles denote $l=0$, and open circles and triangles denote the $l=1$ and $l=2$ components, respectively. The $l=0$ and $l=1$ radii of each atom are joined with a straight line. The numbers 1–5 denote the rows. The first and last atom in each row is indicated.

states of $l=0$ and $l=1$ symmetry approaches unity and $U_l(r)$ becomes approximately l independent. Hence, while for second-row atoms there are two core states of $l=0$ symmetry and only one for $l=1$ symmetry, the pseudopotential cancellation is far better for the former (leading to more delocalized and shallow $l=0$ core potentials), while for the fifth-row atoms the number of core states is 5 and 4, respectively, and the pseudopotential cancellation is very similar for these symmetries. One further notes that while within a given row the slope of the line connecting the $(r_0^{\min}, W_0^{\min})$ and $(r_1^{\min}, W_1^{\min})$ coordinates is negative at the right side of each row (i e., the p potentials are more localized and deeper than the s potential), these slope move gradually towards less negative values and become positive eventually at the left side of the lower rows (i.e., the p potentials become more extended and shallower than the s potentials). This is directly related to the increased delocalization of the outer valence p orbitals as one moves towards the left side of the rows. One notes that the $l=2$ coordinates are quite separated from the $l=0,1$ coordinates, and vary almost linearly within each row. These localized d potentials are responsible for the relatively narrow and separated d bands in the transition-metal series. Their variations along the rows parallels that of the d-band width in the respective elemental metals, and similarly, their proximity to the $l=0$ coordinates governs the degree of s-d hybridization. It is interesting to note that while the decrease in the valence charge Z_v results in relatively more delocalized $l=0,1$ core potentials as one moves to the lighter elements of a given row, the same decrease in Z_v results only in a change in the depths of the $l=2$ potentials, leaving the d-core size of the $4d$ and $5d$ elements relatively unaffected by Z_v.

Figure 7 depicts a $r_0^{\min}, W_0^{\min}$ map for the *columns* in the Periodic Table. Each line connects atoms having the *same* number of valence electrons, denoted by their group number. It is seen that the atoms are grouped naturally according to their chemical behavior: on the lower right side we have the most electronegative atom with its deep and localized potential, while at the upper left side we have the most electropositive atom with its weak and delocalized potential. The first atom of each column (belonging to the first row) is rather separated from the remaining atoms in the same column due to absence of a $l=1$ core state. As the number of valence electrons increases, the potentials tend to span a larger range of depths and a smaller range of radii, while for the low-Z_v elements, the core radius becomes the decisive characteristic feature in a column.[51] Tendencies towards metallization within a given column (e.g., C-Si-Ge-Sn) are reflected by an increased radius and a decreased potential depth (i.e., more free-electron-like).

It is hence seen that the first-principles pseudopotentials faithfully reproduce the regularities of the Periodic Table. We will next examine the degree to which the resulting pseudo-wave-functions parallels the chemical trends in the all-electron wave functions.

IV. FORM OF THE WAVE FUNCTIONS AND THEIR ACCURACY

In order to establish the basis for analyzing the bonding properties of polyatomic systems within the pseudopotential framework, one would like to assure that the atomic pseudo-wave-functions reproduce the pertinent features of the true valence wave functions. One can choose a set of simple prototype systems and examine how well the smooth and nodeless pseudo-orbitals reproduce

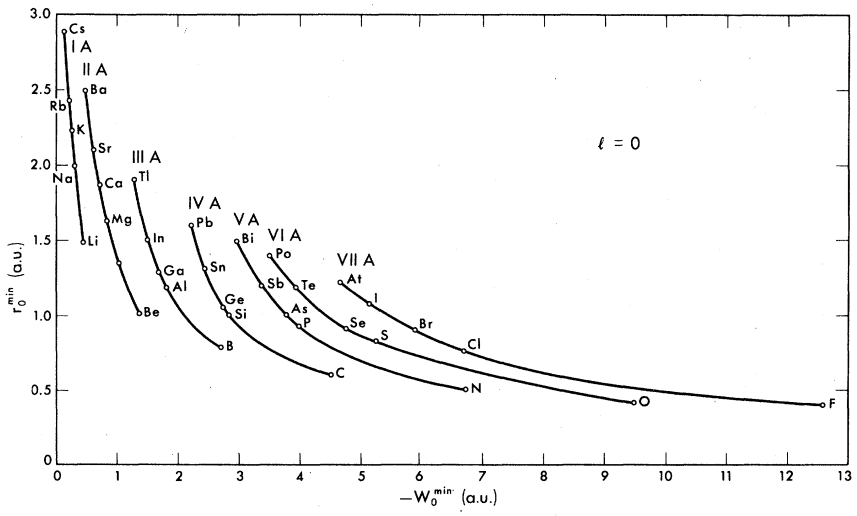

FIG. 7. The $r_0^{\min}$ vs $W_0^{\min}$ coordinates of atoms from columns 1–7. The number of valence electrons is constant along each column, and equals the column number.

the values and regularities in some relevant operator expectation values obtained with the "true" all-electron orbitals. We know that the expectation values of the Hamiltonian operator are, by construction, exactly reproduced for the reference ground state of the atoms. Other operators that might sample the pieces of the wave functions which are relevant to bond formation in condensed systems are r^{-1}, r, r^2, ∇^2, etc. In particular, the various moments of r are useful in depicting the detailed deviations of χ from ψ in the various regions of space, as in a direct comparative plot they are hardly visually distinguishable in the tail regions.

Figures 8–12 show the trends in the moments of r for both the all-electron (full circles) and the pseudo- (open circles) wave-functions for atoms of rows 1–5. Both sets of wave functions were obtained from a self-consistent numerical integration of Eqs. (11) and (8), respectively, with an accuracy of 0.01% in the moments. It is clear that the pseudo-orbitals reproduce the all-electron results to within a few percent, and that even the small variations in the moments within rows in the Periodic Table are directly apparent in the pseudopotential calculation. It is concluded that these pseudopotentials are capable of accurately revealing the chemical trends underlying the all-electron calculations.

A further test for the quality of the pseudo-wavefunctions is furnished by comparing their orbital kinetic energies (which tends to measure the degree of localization of the orbitals) with the corresponding all-electron results. Although the pseudo-orbitals clearly carry less kinetic energy due to the explicit elimination of their radial nodes, one would expect that a chemically meaningful pseudopotential will reproduce the *regularities* in the orbital localization as one moves along rows and columns in the Periodic Table. An example is given in Fig. 13, from which it is evident that this is indeed the case with the presently developed potentials.

The orbital kinetic energies can be further used as a quantitative measure of the pseudopotential cancellation for each angular-momentum species. The ratio $f_l = T^{nl}_{\rm PS}/T^{nl}_{\rm AE}$, (where T^{nl} stands for the orbital kinetic energy per electron and PS and AE denote, respectively, pseudopotential and all-electron) equals 1.0 when the pseudopotential transformation (12) does not modify the wave function (i.e., l not present in the core), and decreases towards zero as the degree of kinetic energy cancellation increases. We find that to within a good approximation, f_l is constant within rows in the Periodic Table, indicating that it is the number of radial nodes rather than the core charge that determines the degree of pseudopotential cancellation. Although the variations from constancy of f_l may admittedly reflect genuine chemical trends, these deviations are very small and can be ignored for the purpose of the present discussion. Table I gives the values of f_l with their characteristic variance, as calculated for all atoms of rows 1–5. It is seen that the $l=0$ cancellation is always about a factor of 2 better than the $l=1$ cancellation, while the $l=1$ cancellation is better to within a similar factor than the $l=2$ cancellation. Further, even for a constant number of core states of the

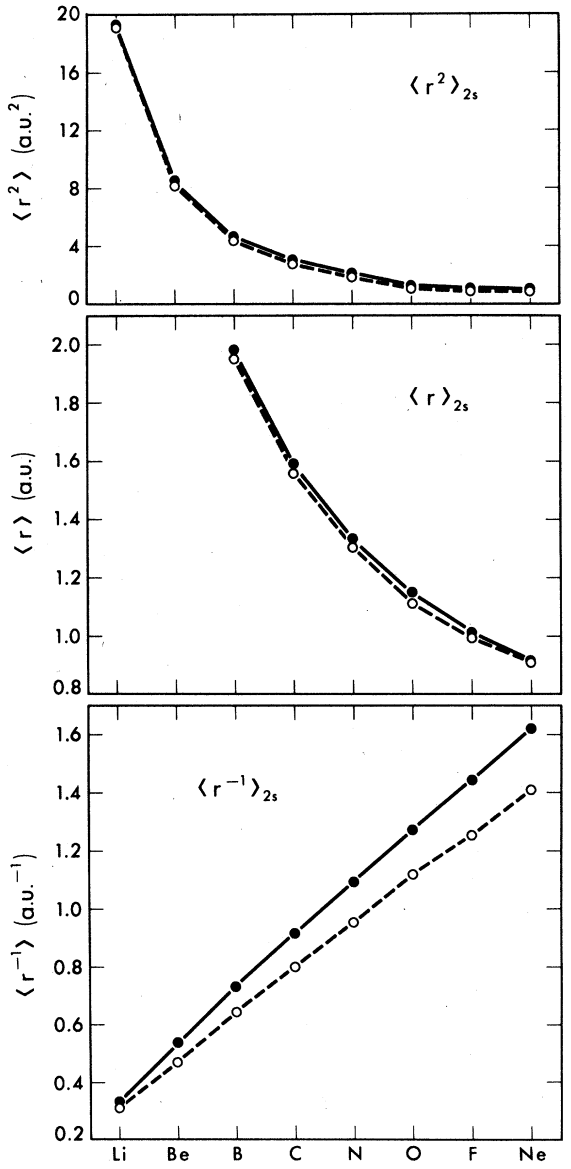

FIG. 8. Orbital moments for the valence electrons of the first-row atoms. Full and open circles denote all-electron and pseudopotential results, respectively. The 2*p* orbital moments are identical by definition.

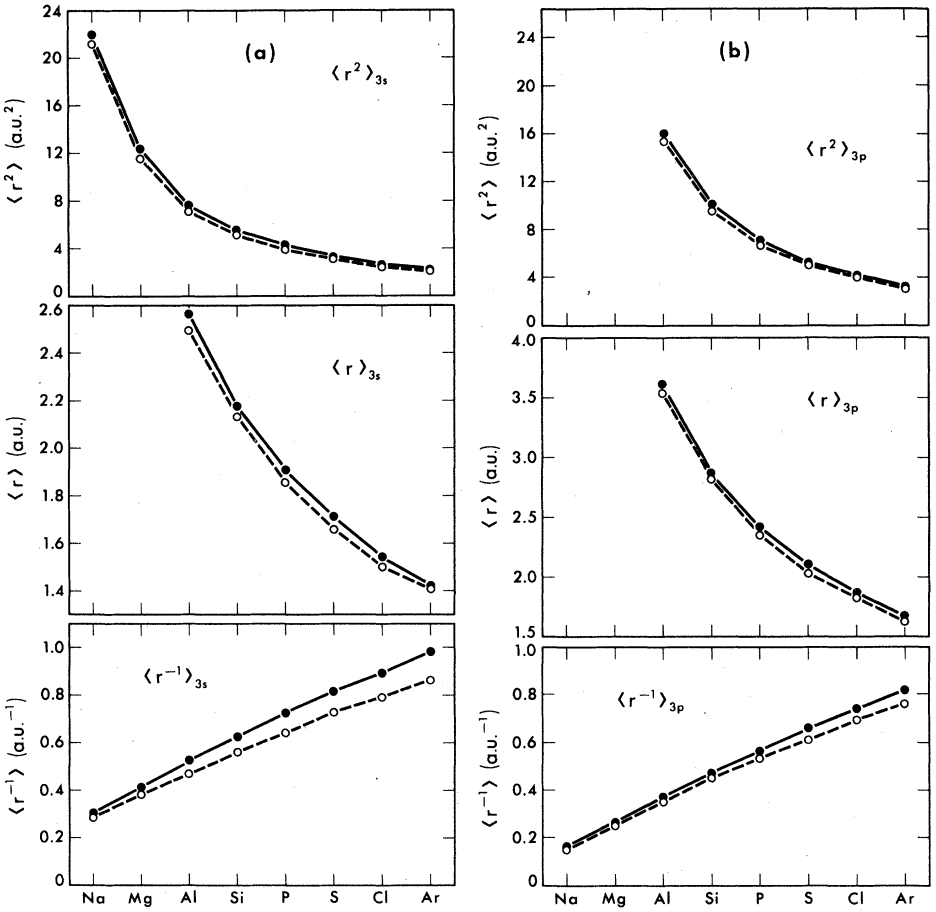

FIG. 9. Orbital moments for the valence electrons of the second-row atoms. Full and open circles denote all-electron and pseudopotential results, respectively. (a) $3s$, (b) $3p$. The $3d$ orbital moments are identical by definition.

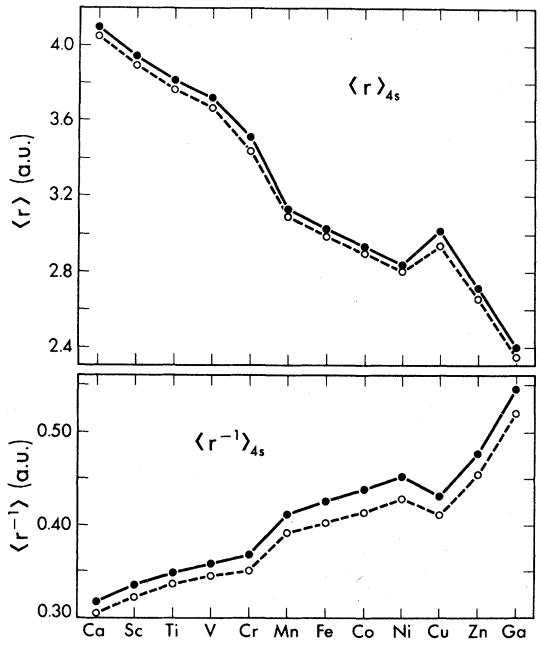

FIG. 10. Orbital moments for the $4s$ states in the first-row transition atoms. Full and open circles denote all-electron and pseudopotential results, respectively.

appropriate symmetry, the order of improved cancellation remains $l=0>l=1>l=2$. Clearly, the constancy of the orbital kinetic energy ratios within rows reflects the fact that the pseudopotential transformation we used retains the regularities of the orbital localization present in the all-electron picture. In contrast, there is no guarantee that the wave-function systematics would be preserved in either the model potential approach[3,26-33] or the Phillips-Kleinman[20] approach. Unless special care is taken, these wave function need not reflect the characteristic features of the true orbitals.

Still a different measure of the quality of the pseudo-wave-functions is provided by the calculated x-ray scattering factors $F(Q)$. We find that the deviations of the pseudopotential atomic scattering factors from the corresponding quantity computed with the true valence orbitals does not exceed 2%, and is very small relative to the number of valence electrons. Some typical examples are given in Fig. 14(a), where the core charge density was simply added to the valence pseudo-charge-density in calculating $F(Q)$. The errors are seen to be located almost equally at low and

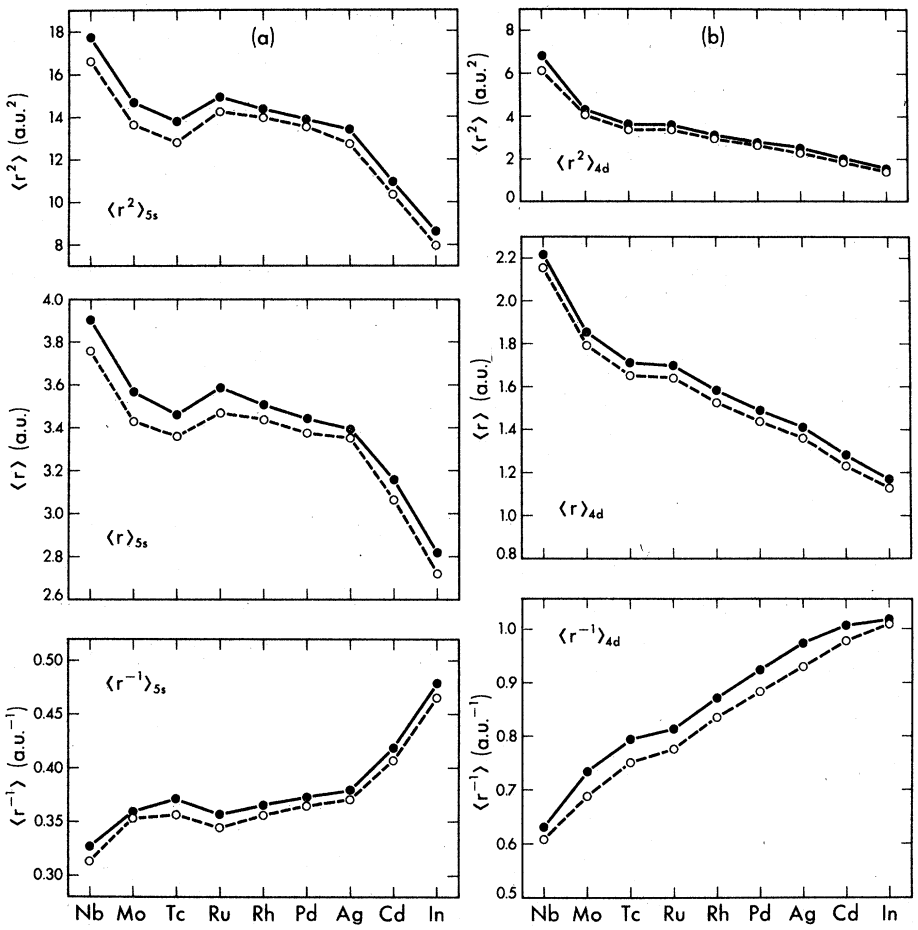

FIG. 11. Orbital moments for the valence electrons of the second-row transition metals. Full and open circles denote all-electron and pseudopotential results, respectively. (a) 5*s*, (b) 4*d*.

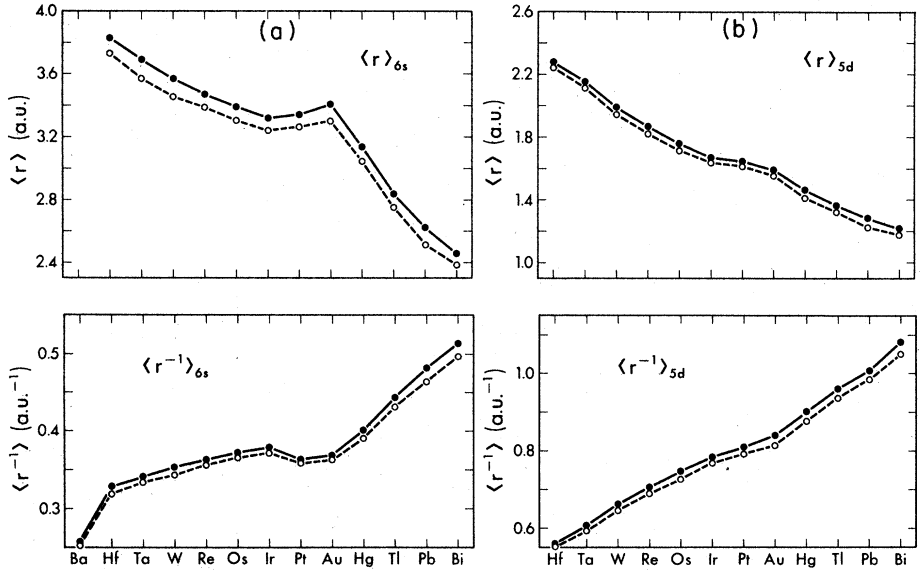

FIG. 12. Orbital moments for the valence electrons of the third-row transition metals. Full and open circles denote all-electron and pseudopotential results, respectively. (a) 6*s*, (b) 5*d*.

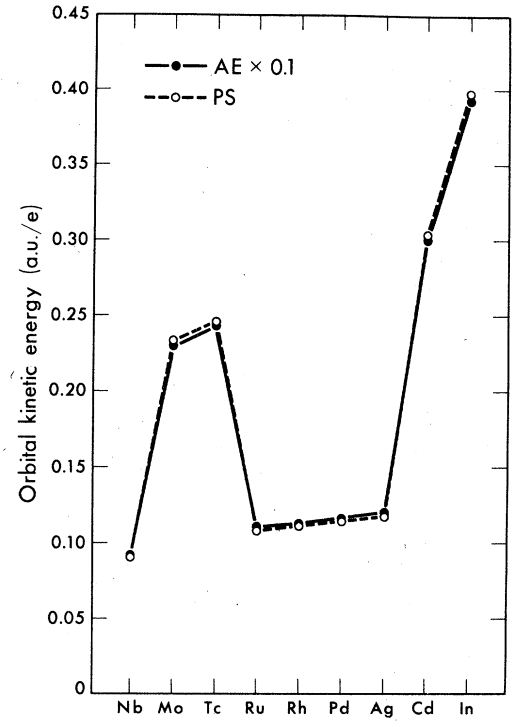

FIG. 13. Comparison of the 5*s* orbital kinetic energy per electron of the fourth-row atoms obtained in the all-electron (●) and pseudopotential (○) calculation. The all-electron results are multiplied by a factor of 0.1.

high momentum [Fig. 14(b)], and are in general within the experimental accuracy of most measurements. We emphasize that within the first-principles pseudopotential scheme developed here, an orthogonalization of the valence pseudo-orbitals to the core wave function results in the exact valence orbitals (for the reference atomic ground state), and hence the errors in the moments $\langle r^\lambda \rangle$ and x-ray scattering factors vanish *identically*. This does not occur in the model potential formulations, where it is found that core orthogonalization results sometimes in even larger deviations from the all-electron results.[52]

TABLE I. Kinetic energy cancellation factor $f_l = T^{nl}_{PS}/T^{nl}_{AE}$ for the first five rows in the Periodic Table. The core orbitals in the ith row are defined as the rare-gas configuration of the $i-1$ row.

Row	f_s	f_p	f_d
1	0.78 ±0.01	1.00	1.00
2	0.175±0.02	0.39 ±0.03	1.00
3	0.135±0.002	0.29 ±0.03	1.00
4	0.102±0.002	0.235±0.04	0.50±0.02
5	0.083±0.005	0.185±0.03	0.36±0.02

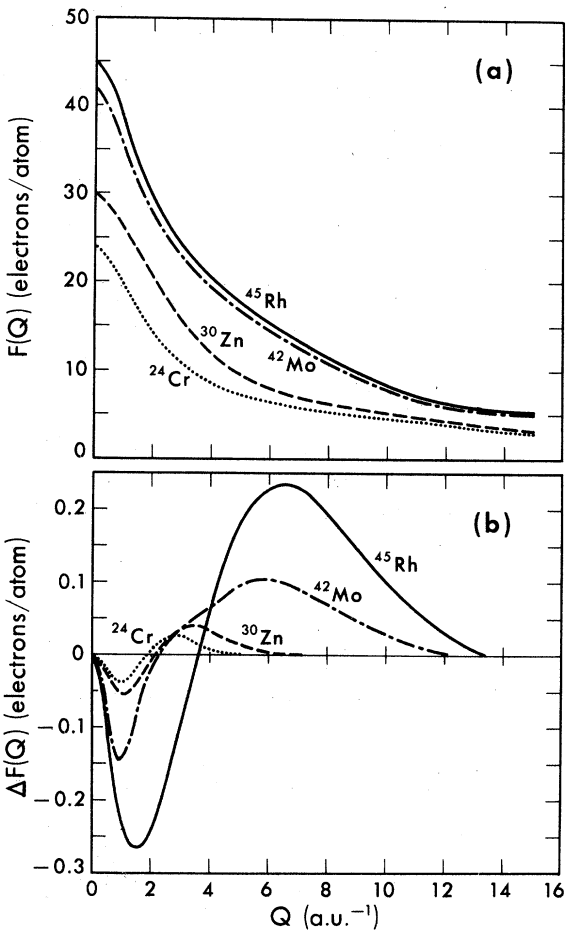

FIG. 14. (a) X-ray atomic scattering factors of Cr, Zn, Mo, and Rh, calculated from the pseudo-valence-charge-density plus the all-electron core density. $F(Q=0)$ is normalized to the atomic number. (b) The difference between the exact all-electron atomic scattering factor and that calculated from pseudo-wave-functions as a function of momentum. Note that in the present formalism this difference vanishes identically when the pseudo-wave-functions are core orthogonalized.

V. ENERGY DEPENDENCE OF THE POTENTIALS

The pseudopotential partitioning of the effective field seen by a valence electron into a static core potential $\sum_l W_l(\vec{r})\hat{P}_l$ and a dynamic valence response potential $V_{ee}(n(\vec{r}))+V_{xc}(n(\vec{r}))$ are useful to the extent that the former is genuinely transferable from the prototype electronic configuration to arbitrary systems. One would expect this transferability to hold to the extent that the core characteristics as well as the core-valence interactions of given angular momentum symmetries are similar in both systems. In these cases the valence field $V_{ee}(n(\vec{r}))+V_{xc}(n(\vec{r}))$ readjusts dynamically (via a self-consistent treatment) to screen the to-

tal core potential $W_{tot}(\vec{r})$ such that the resulting variational density parallels the all-electron density obtained in the presence of the simpler $-Z/r$ static external potential. Note that in contrast to the empirical model potential[3,26,27] approach in which the entire *effective potential* is considered as the transferable unit, the present approach used only the *atomic core potential* as the system-invariant unit, and allows for a system-dependent self-consistent screening through the valence response potential. Although the ultimate test for the transferability of the core potentials should be based on actual quantitative comparisons of all-electron and pseudopotential calculations for polyatomic systems (to be presented in a separate paper),[52] a good idea of the stability of a given pseudopotential against various bonding perturbations can be obtained simply by considering excited and ionized states of the atom. Although restricted to spherical site symmetries, these excited states offer a large range of variations in both wave functions and energies so that the capability of the potential in reproducing the all-electron results over a sizable energy range in the polyatomic system can be judged. One would expect a pseudopotential to successfully replace the actual dynamic effects of the core electrons in some energy range ΔE_t above the reference state used for its construction. In this simple case the question of transferability of the potential from one electronic state to the other reduces to its degree of energy dependence; the potential is said to be approximately energy independent over the range ΔE_t if it reproduces the all-electron results over this range. One is typically interested in probing the stability of the potential for excited atomic configurations that can be actually mixed into the states of interest in the condensed system, say, over one to two valence-

TABLE II. Tests for the stability of the Mn ground-state pseudopotential against electronic excitations. Energies are given in eV and moments in a.u. AE, PS, and PS-ortho. denote, respectively, all-electron, pseudo, and core-orthogonalized pseudo.

	ϵ_{3d}	ϵ_{4s}	ϵ_{4p}	ΔE_t	$\langle r\rangle_{3d}$	$\langle r\rangle_{4s}$	$\langle r\rangle_{4p}$
			$Mn^0\ 3d^5 4s^2 4p^0$				
AE	− 5.994	− 4.264	− 0.776	0.000	1.225	3.173	4.915
PS	− 5.994	− 4.264	− 0.776	0.000	1.225	3.074	4.895
PS-orth.						3.173	4.915
			$Mn^0\ 3d^6 4s^1 4p^0$				
AE	− 2.634	− 3.385	− 0.430	− 0.626	1.392	3.412	5.867
PS	− 2.685	− 3.410	− 0.461	− 0.619	1.394	3.381	5.689
PS-orth.						3.408	5.806
			$Mn^0\ 3d^5 4s^1 4p^1$				
AE	− 7.603	− 5.301	− 1.517	3.401	1.207	3.065	4.453
PS	− 7.615	− 5.331	− 1.531	3.402	1.206	2.998	4.387
PS-orth.						3.053	4.424
			$Mn^+\ 3d^6 4s^0 4p^0$				
AE	− 9.814	− 9.642	− 5.694	6.013	1.316	3.003	3.895
PS	− 9.915	− 9.681	− 5.631	6.106	1.320	2.972	3.803
PS-orth.						2.998	3.870
			$Mn^+\ 3d^5 4s^1 4p^0$				
AE	−13.991	−11.000	− 6.524	7.537	1.191	2.856	3.605
PS	−14.026	−11.109	− 6.605	7.600	1.190	2.781	3.558
PS-orth.						2.846	3.598
			$Mn^+\ 3d^4 4s^2 4p^0$				
AE	−19.321	−12.561	− 7.566	12.326	1.093	2.697	3.328
PS	−19.400	−12.604	− 7.603	12.341	1.089	2.599	3.284
PS-orth.						2.685	3.314
			$Mn^{+2}\ 3d^5 4s^0 4p^0$				
AE	−23.254	−18.377	−13.038	22.230	1.152	2.623	3.123
PS	−23.591	−18.435	−13.204	22.435	1.151	2.585	3.094
PS-orth.						2.604	3.100

band widths of the solid. Clearly, if one wants to study different energy regions in the condensed phase (e.g., outer-core states or highly excited Rydberg states), one would have to construct a new potential based on a different electronic reference state such that the stability range ΔE_t would cover the relevant energy region (cf. Sec. VI).

We have performed numerous tests on the stability of the first-principles pseudopotentials in the atomic limit. Typical examples are given in Tables II and III, in which we summarize the resulting eigenvalues, total energy differences ΔE_t (relative to the reference state), and orbital moments obtained both with the pseudopotential and the all-electron calculations. The accuracy in determining the energy eigenvalues and total energies in the self-consistent numerical integration scheme is of the order of 3.10^{-6} eV. It is seen that the ground-state pseudopotential, which exactly reproduce the eigenvalues of the reference state (e.g., Mn^0 $3d^5 4s^2 4p^0$), accumulates only small errors as ΔE_t is raised to about 22 eV above the ground state. Likewise, the description of the valence wave functions remains accurate over a range of 2%–40% of variation in the orbital moments. The worst case in Table II is the highly excited Mn^{2+} configuration ($\Delta E_t = 22$ eV), for which the errors in the eigenvalues are 0.2–0.4 eV, or 1%–2%; however, this configuration is hardly of relevance for the states around the Fermi level in the metal. In general, we find that a neutral-atom potential is stable until roughly two or more of its electrons are ionized. Above this limit the core is already appreciably modified for the underlying frozen-core approximation to be valid. We note that many of the empirical and semiempirical model potentials previously employed have used the observed excitation energies of the *single-valence-electron* ions as basic input for fitting the potentials.[12,24,29,32,33,47,48] While these procedures involve the considerations of only low excited states for the first columns of the Periodic Table, their application to the right-side part of the Table actually implies the extension of the frozen-core approximation to wide energy regions (e.g., 152 eV for Nb^{5+}). These highly excited states are usually characterized by wave functions that are substantially different from those pertaining to the vicinity of the ground state (e.g., in going from Nb^0 to Nb^{5+}, the orbital kinetic energies per electron vary by 26 and 34 eV for the $4s$ and $4p$; the $5s$, $5p$ orbital moments vary by 34% and 46%, respectively, etc.) and their use in fitting the potential might induce an unwarranted energy dependence. Indeed, some workers[53] have found that it is sometimes necessary to rescale the Hamiltonian matrix elements when such as ionic potential is used, in order to get agreement with the all-electron results.

Tables II and III also indicate the effect of orthogonalizing the valence pseudo-wave-functions to the (frozen) ground-state core orbitals. It is evident that this yields remarkably improved accuracy

TABLE III. Tests for the stability of the Ge ground-state pseudopotential. Energies are given in eV and moments in a.u. AE, PS, and PS-orth. denote, respectively, all-electron, pseudopotential, and core-orthogonalized pseudopotential results.

	ϵ_{4s}	ϵ_{4p}	ΔE_t	$\langle r\rangle_{4s}$	$\langle r\rangle_{4p}$
		Ge^0 $4s^2 4p^2$			
AE	−10.524	− 3.121	0.000	2.101	2.973
PS	−10.524	− 3.121	0.000	2.081	2.944
PS-orth.				2.101	2.973
		Ge^0 $4s^1 4p^3$			
AE	−11.430	− 3.747	7.564	2.119	2.844
PS	−11.441	− 3.751	7.559	2.093	2.771
PS-orth.				2.118	2.841
		Ge^{+1} $4s^2 4p^1$			
AE	−18.490	−10.369	6.612	2.069	2.591
PS	−18.601	−10.421	6.661	1.998	2.550
PS-orth.				2.061	2.571
		Ge^0 $4s^1 4p^2 4d^1$			
AE	−15.893	− 7.601	13.414	2.049	2.575
PS	−15.892	− 7.621	13.392	1.988	2.558
PS-orth.				2.039	2.574

in the moments over a wide energy range; while the pseudo-wave-functions are usually characterized by smaller first-moments due to their core components [Eq. (12)], the orthogonalization procedure annihilates these states, the remaining discrepancies being due to small deviations from the frozen-core approximation.

A different way of examining the stability of the first-principles pseudopotentials involves their generation from a set of reference states and their subsequent application to a given test state. For example, one can generate a potassium potential from a number of configurations of the form $K\ 4s^Q 4p^{1-Q}$ with $0 \leq Q \leq 1$, and test their accuracy in reproducing the characteristics of the ground state ($Q = 1$). We find that the errors introduced in the calculated energy eigenvalues and orbital moments are less than 0.02 eV and 1%, respectively, indicating a low energy dependence. We conclude that the presently developed pseudopotentials can be used to replace the core electrons in a wide variety of bonding situations spanning large ranges of orbital localization.[54]

VI. DIFFERENT CORE-VALENCE SEPARATION SCHEMES

In constructing the pseudopotentials (Figs. 1–5), we have so far adopted the classical chemical definition of core versus valence orbitals (the former belonging to the nearest rare-gas closed shell). Although this definition underlies much of the chemical periodicities, it is by no means unique; the partitioning of the all-electron states into the "passive" and the "active" subgroups can be based on their response to relevant external perturbations. An example for the type of considerations involved in invoking such a partitioning is given in Fig. 15, where we plot the variation in the all-electron energy eigenvalues and kinetic energies

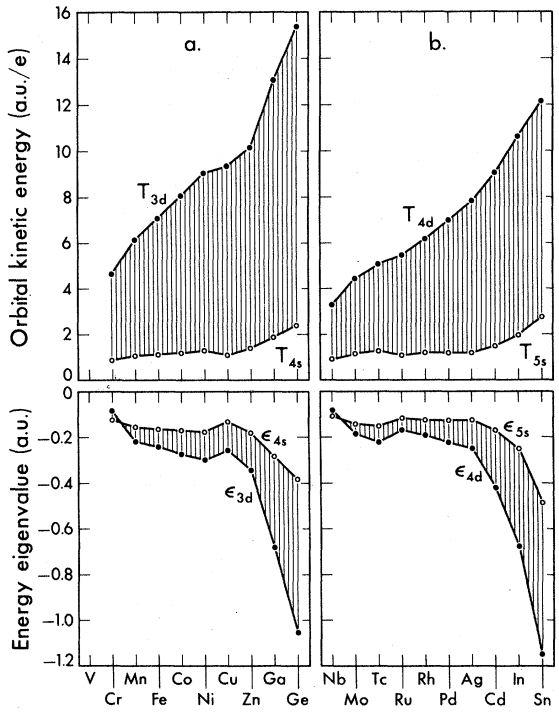

FIG. 15. All-electron energy eigenvalue gap $\epsilon_s - \epsilon_d$ and the orbital kinetic energy per electron gap $T_s - T_d$ of the outer orbitals of the (a) third-row and (b) fourth-row atoms.

of the outermost s and d electrons for atoms of rows 3 and 4. It is seen that while at the left-hand side of each row the $\epsilon_s - \epsilon_d$ energy gap is very small and the corresponding degrees of localization of the orbitals are not too different, the right side of these rows is characterized by large differences in the one-electron energies and kinetic energies, making s-d hybridization less likely. On this basis one would assume that for suffic-

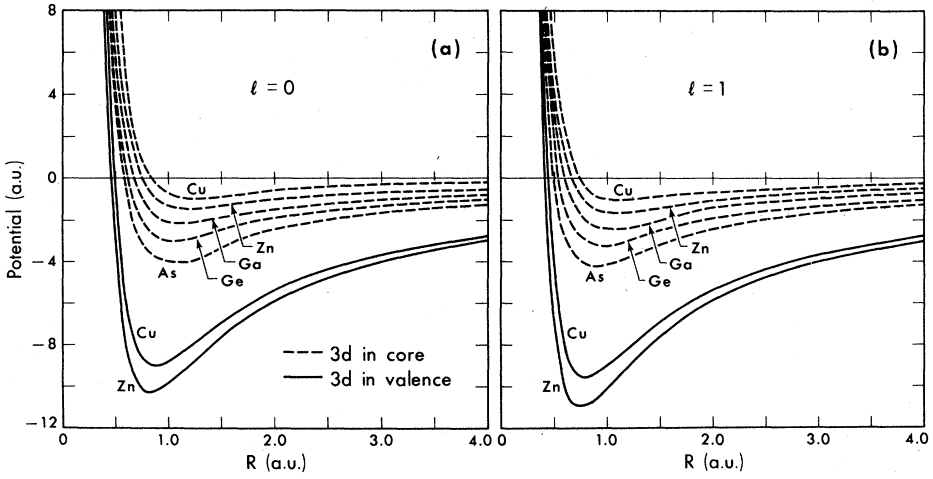

FIG. 16 Atomic core potentials of the third-row atoms computed with the $3d$ orbitals as a part of the core (---) and as a valence states (—). (a) $l = 0$, (b) $l = 1$.

iently low energy bonding (or external) perturbations, the outer d states of, say, Zn, Ga, Ge, In, and Sn can be considered as part of the inert core. The first-principles pseudopotential scheme developed here provides the flexibility of constructing the core potentials for various core-valence partitioning schemes, since the only invariant quantity for a given choice of the nodeless valence orbitals in (12) is the *total effective* potential in Eq. (5), and not its components. Clearly, adding a given set of orbitals as a part of the core would result in different core potentials in Eq. (19); the accompanying changes in the screening field would, however, lead to a similar effective potential, provided the principal quantum numbers of the lowest valence orbitals are unchanged. We next examine here the potential usefulness of such core redefinitions.

Figure 16 shows the $l=0,1$ components of the atomic core potentials of Cu, Zn, Ga, Ge, and As computed with the $3d$ orbitals as a part of the core (dashed lines). For comparison, we give in the same figures the Cu and Zn potentials computed with the $3d$ as a part of the valence shell (full lines). It is seen that incorporation of the $3d$ orbitals into the core results in much shallower s and p potentials. The core potentials of Ga, Ge, and As are now more in line with those of Al, Si, P, etc. The association of the Ga-Ge-As compounds with the other "covalent" systems of columns III–V rather than with the transition series is hence based on the passivity of their $3d$ electrons to hybridization with the s,p states, and is clearly revealed in their corresponding core potentials.

The incorporation of the $3d$ orbitals into the core results in two additional effects: (i) the nonlocality of the $l=0,1$ core potential is enhanced, i.e., $W_0(r)-W_1(r)$ increases in magnitude in the region 0.8 a.u. $\lesssim r$. In general, one expects such nonlocality enhancements whenever the valence subspace is reduced, and conversely, a gradual approach to a fully local potential is obtained as more of the states are treated by a dynamic response $V_v(r)$ rather than by a static pseudopotential.[37] Clearly, at the limit where all states are treated by $V_v(r)$ (the all-electron limit), all angular momentum species experience the same local potential (in the local-density formulation). (ii) The energy dependence of the potential increases, i.e., the new core potential is expected to be stable only in the perturbation energy ranges that leave the $3d$ orbital unchanged relative to the reference state.

From the practical point of view, the use of these pseudopotentials with a redefined core poses some attractive features. For example, methods that employ a reciprocal space expansion of $W_l(r)$ becomes more readily convergent with shallower potentials (i.e., require fewer plane waves). The added nonlocality does not pose serious difficulties, since most of it is localized in the regions of space where the valence state changes very little upon bond formation.

Similar arguments pertain to the $4f$ electrons in the fifth row in the Periodic Table. Their inclusion as a part of the valence in tungsten results in a deep core potential (with $W_s^{\min}=-2.8$ a.u., $W_p^{\min}=-2.74$ a.u., $W_d^{\min}=-11.8$ a.u., and $r_s^{\min}=1.56$ a.u., $r_p^{\min}=1.64$ a.u., and $r_d^{\min}=0.51$ a.u.). It is hence clear from the foregoing discussion that the choice of a core-valence partitioning scheme in the present formalism is largely arbitrary, and can be carried out to suit particular applications and the desired accuracy.

VII. IMPROVEMENTS AND GENERALIZATION OF THE UNDERLYING INTERACTION MODEL

We have seen so far that the first-principles local-density pseudopotential approach reproduces the properties of the all-electron solutions remarkably well, over large energy ranges. Since we have adopted a completely nonempirical approach, we expect these potentials to similarly carry over the major disadvantages and shortcomings of the underlying all-electron interaction model. Numerous applications of the all-electron local-density formalism to the description of structural and electronic properties of molecules[55,56] and solids[57-61] have yielded excellent results for ground-state properties such as cohesive energy, bond length and equilibrium unit-cell parameters, bulk modulii, x-ray scattering factors, etc. Its major shortcoming lies in the lack of a simple correspondence between the associated energy eigenvalues and the actual electronic elementary excitations in the system.[43,61-63] Viewed from a slightly different point, while the eigenvalues of the HF equations correspond rigorously to the difference in *total* energies of the ionized system and the ground-state system at the limit of no orbital relaxation (Koopman's theorem) and hence can be used as reference points for analyzing the observed ionization spectra and, in general, the calculated one-electron spectra of solids, no such theorem holds for the local-density Hamiltonian. The implications of this situation from the theoretical point of view are that the conventional local-density one-electron band model does not represent the actual independent-particle states. From the practical point of view, one finds that if the predictions of the local-density model are not obscured by empirical parametri-

zations or systematic adjustments, the resulting band gaps of insulators are often too small by 20%–30% compared to optical data (notable examples are LiF,[61] Si,[52] CdS,[58] and many rare-gas solids[64]), the d-band width of transition metals is 15%–25% off the observed photoemission data,[65] and that the negative of the atomic eigenvalues are in error by a similar amount from the observed ionization photoelectron spectra.[43,62] Quantitative analysis of these effects[61,62] suggests that a major part of these discrepancies arise from the noncancellation of the Coulomb and exchange self-interactions in the local-density model; while both the Hartree and HF models provide explicitly for a cancellation of these unphysical interactions, the local-density model treats the electronic Coulomb and exchange self-interactions in a state-independent (local) fashion, which results in only a partial compensation of the self-interactions. An obvious example is the hydrogen atoms,[66] for which in the LDF model the entire "interelectronic" Coulomb and exchange potentials $V_{ee}+V_x$ are due to the spurious self-interactions. The partial success of the local-density model in interpreting one-electron spectra of solids is largely due to the fact that in extended electronic states, the self-interaction effects are often small (inversely proportional to the number of particles. While this condition holds for many of the free-electron-like metals, many of the electronic states in transition metals, insulators, and semiconductors do maintain some degree of spatial localization, resulting in nonnegligible self-interaction corrections. This deficiency of the local-density model is quite often dealt with in atoms or simple molecules by evaluating directly the *total* energy differences between ground and excited states [via the "transition state"[43] or direct ΔSCF (change in self-consistent-field energy, in which the threshold energy is taken as the difference in total energies of two self-consistent-field calculations)[61,67] calculations] and by inclusion of spin-polarized electron-liquid correlation terms[66] that act to partially offset these deviations. With only few exceptions, similar methods are extremely difficult to carry over to the study of solids. We propose here a partial solution and simplification of the problem within the first-principles pseudopotential model. We will later discuss the possibility of further generalizations of the LDF model within the pseudopotential context.

One first realizes that the noncancellation of the self-interactions in the LDF model stems from the local nature of the corresponding all-electron potential $V_{\rm tot}(\rho(\vec{r}))$; as the self-interaction

$$V_{\rm SI}^{(i)}(r)=\int \frac{\psi_i(r')\psi_i^*(r')}{|r-r'|}\,dr'+V_x(\psi_i(r)\psi_i^*(r)) \qquad (22)$$

is explicitly state dependent, it is not representable in a conventional local model. One expects this term to dominate the calculated spectra of one-electron atoms or that of systems for which $\psi_i(r)\psi_i^*(r)$ has appreciable magnitude over small regions of space. While in the *all-electron* model the first case is realized only for the hydrogen atom, the first case appears in many more situations in the *pseudopotential* model (e.g., the entire first column, Cu^+, etc.). We illustrate this in Table IV, where we compare the calculated pseudopotential atomic total energies $E_{\rm tot}^{\rm PS}$ of the first-column atoms, with the observed ionization potentials[68] IP(exp). Since these pseudoatoms are one-electron systems, their total pseudopotential energy is expected to represent the interaction of the electron with the core, and hence to be comparable to the ionization energy. One finds, in turn, a roughly constant deviation Δ_1 from the observed value of 15%–20%. These deviations result both from the fact that the electron is allowed to spuriously interact with itself, and from the incompleteness of the correlation interaction underlying the local-density pseudopotential.

A straightforward treatment of the self-interaction can be achieved through its direct cancellation in the all-electron potential.[69] Hence one treats all the *interelectronic exchange* interactions statistically via the standard local-density formalisms, while the *self-exchange* is treated separately in the spirit of the Hartree approach. This results

TABLE IV. Total pseudopotential energies of the alkali atoms, compared with the observed ionization potentials (Ref. 68). $E_{\rm tot}^{\rm PS}$ and $E_{\rm tot}^{\rm PS,SIC}$ are, respectively, the local-density and self-interaction cancelled pseudopotential total energies (in eV). Δ_1 and Δ_2 are the percent deviations of $E_{\rm tot}^{\rm PS}$ $E_{\rm tot}^{\rm PS,SIC}$ from the observed values, respectively.

Atom	$-E_{\rm tot}^{\rm PS}$	IP(exp)	Δ_1	$-E_{\rm tot}^{\rm PS,SIC}$	Δ_2	HF, ΔSCF[70]
Li	4.504	5.39	16.4%	5.341	0.91%	5.34
Na	4.361	5.14	15.1%	4.982	3.1%	4.95
K	3.635	4.34	16.2%	4.103	5.5%	4.00
Rb	3.458	4.18	17.3%	3.910	6.5%	3.81
Cs	3.138	3.89	19.3%	3.598	7.5%	•••

in a nonlocal exchange potential of the form

$$V_x^{(nl)}(\rho(r), \tilde{\psi}_{nl}(r)) = V_x(\tilde{\rho}(r)) - V_{SI}^{(nl)}(\tilde{\psi}_{nl}(r)) \quad (23)$$

and the corresponding state-dependent total potential

$$V_{tot}^{(nl)}(\tilde{\rho}(r), \tilde{\psi}_{nl}(r)) = -Z/r + V_{ee}(\tilde{\rho}(r)) + V_x^{(nl)}(\tilde{\rho}(r), \tilde{\psi}_{nl}(r)). \quad (24)$$

This form has been suggested by Lindgren[69] and applied in the all-electron context to the Cu^+ ion. Clearly, this considerably complicates the solution of the all-electron problem due to the need to solve a self-consistently coupled state-dependent problem. However, since the pseudopotential transformation of even a *local* all-electron Hamiltonian [e.g., Eq. (11)] results in an angular-momentum-dependent nonlocal core potential (19), one might make use of the fact that the nonlocality in Eq. (24) is of similar orbital nature and generate a self-interaction compensated pseudopotential with no additional complexity over the regular pseudopotentials.

Proceeding along the lines outlined in Sec. II, one performs a similar pseudopotential transformation on the potential (24), characterized by the eigenstates $\tilde{\psi}_{nl}(r)$. The resulting core potential is

$$S_l(r) = \tilde{W}_l(r) + \left[\tilde{V}_x^{(nl)}(r) - \left(\sum_{n'} \tilde{C}_{n'l,nl} \tilde{V}_x^{(n'l)}(r) \tilde{\psi}_{n'l}(r)\right) \Big/ \left(\sum_{n'} \tilde{C}_{n'l,nl} \tilde{\psi}_{n'l}(r)\right)\right], \quad (25)$$

where quantities marked by a tilde indicate that they are computed from the nonlocal all-electron problem, with potential (24), and $\tilde{W}_l(r)$ has the same form as in Eq. (19). This self-interaction compensated core potential is different from the original form (19), both in the occurrence of modified wave functions $\tilde{\psi}_{nl}(r)$ in the regular core potential form $\tilde{W}_l(r)$, and in the new term (in large square brackets), which measures the difference between the valence exchange self-interaction term $\tilde{V}_x^{(nl)}(r)$ and the configurational average core-valence self-interaction.

Table IV shows the resulting pseudopotential total energies $E_{tot}^{PS,SIC}$ computed with this modified core potential. They are also compared with the ΔSCF (total energy differences) results obtained from an all-electron HF calculation.[70] One observes that a large part of the discrepancy which existed between the observed ionization potentials and the previous pseudopotential calculation has been eliminated. The new results are somewhat better than the HF results, and show now a smaller but *systematic* error which increases with atomic number, much like the trends in the HF results. Since the HF ΔSCF results include the effects of orbital relaxation and are performed with high accuracy, the remaining differences with experiment reflect correlation corrections. The next step in improving the pseudopotentials would hence have to deal with correlation effects in the all-electron representation. Before commenting on this possibility, we will further examine the implications of the self-interaction corrections on the core potentials.

Figure 17 shows the state-dependent exchange potential (23) multiplied by r for the various orbitals of Li, compared with the usual local-exchange $rV_x(\rho(r))$. The marked difference between the two types of the exchange potentials is that the self-interaction corrected one approaches $-1/r$ at large distances from the origin (as expected electrostatically), while the regular local-exchange potential decays to zero much faster because of its self-interaction terms.

The nonlocality of the exchange is seen to be most pronounced for the more localized 1*s* core state and decreases for the more diffused 2*s* and 2*p* valence orbitals. We have shown that the pseudopotential approach to the self-interaction compensated problem results in a significant simplification over the corresponding all-electron problem in that only the valence states have to be treated by a nonlocal screening field, while the core nonlocality is absorbed into the usual pseudopotential nonlocality. The fact that most of the exchange nonlocality is carried by the more localized core states suggests a simplifying approximation. One can still approximately treat the valence field in Eq. (5) in a local fashion, and include all the essential nonlocalities simply by using the modified core potentials $S_l(r)$. This approach should enable a much better characterization of the localized nature of narrow *d* bands in transition metals as well as the valence bands of the alkali-halides and

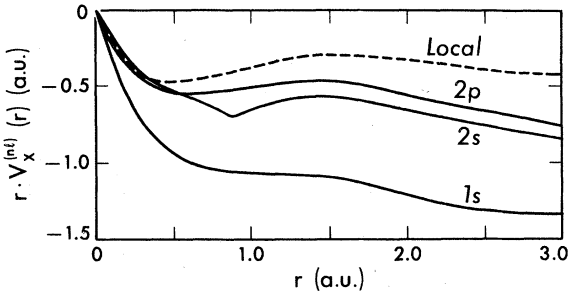

FIG. 17. r times the nonlocal all-electron exchange potential of the various orbitals in the Li atom (full lines) compared with the density functional local form (broken line).

TABLE V. Energy eigenvalues and orbital moments (in a.u.) for Cu^+ obtained with the LDF and self-interaction compensated (SIC) LDF potential, compared with HF results.

	LDF	HF (Ref. 70)	SIC LDF
ϵ_{1s}	−321.02	−329.11	−330.10
ϵ_{2s}	− 38.38	− 41.13	− 40.04
ϵ_{2p}	− 33.74	− 35.93	− 35.77
ϵ_{3s}	− 4.32	− 5.32	− 4.82
ϵ_{3p}	− 2.87	− 3.64	− 3.36
ϵ_{3d}	− 0.47	− 0.81	− 0.81
$\langle r\rangle_{1s}$	0.053		0.053
$\langle r\rangle_{2s}$	0.239		0.238
$\langle r\rangle_{2p}$	0.208		0.206
$\langle r\rangle_{3s}$	0.725		0.724
$\langle r\rangle_{3p}$	0.756		0.753
$\langle r\rangle_{3d}$	1.017		0.949

rare-gas solids by taking account of a sizable part of intrasite Coulomb and exchange interactions.

The self-interaction compensated exchange potential is in general more attractive than the local exchange (Fig. 17) and leads to more tightly bound states. The energy eigenvalues are now more in line with the HF results, as can be seen from Table V for Cu^+.[71] The largest effects are observed for the localized core states, as discussed above. The resulting wave functions tend similarly to be more localized. Note that both these effects tend to produce a more localized core potential with smaller classical turning point radii r_l^0. We find, however, that the effect on the radii r_l^0 is much smaller for many-valence electron atoms, and hence in our applications of these radii for partitioning of structural phases of crystals[50] we use the modified radii only for the alkali atoms.

We close this section by commenting on possible improvements of the correlation functional in the pseudopotential problem. The need for these improvements is apparent in the systematic deviations shown in Table IV and in the similar deviations observed in the past[66,72] between the local-density and the exact exchange energies. Although the explicit treatment of the self-interaction already results in a marked improvement in the calculated total exchange energy (i.e., in Li, the LDF result is −1.4805 a.u., as compared to the exact HF value[72] of −1.7385 a.u. and our self-interaction corrected value of −1.6805 a.u.), it has been shown[66] that when the spin-polarized electron-liquid correlation functional is used instead of the simpler $\rho^{1/3}$ local exchange, a systematic partial cancellation of errors occurs. Although outside the scope of the present work, it would seem that such corrections could be easily incorporated into the first-principles core potential along the lines outlined in Sec. II. This would result in a spin- and angular-momentum-dependent core potential, and would enable first-principles studies of magnetic problems within the pseudopotential framework. Similar comments apply to the inclusion of gradient corrections to the correlation[45] in the total all-electron potential and its corresponding core potentials. We have incorporated the homogeneous electron-liquid non-spin-polarized correlation functional of Singwi *et al.*[44] into our pseudopotential formalism, and calculated the corresponding core potentials self-consistently for few atoms. We find that the general effect is to somewhat localize these potentials (e.g., the turning points r_l^0 for carbon are reduced by 1% and 2% for $l=0$ and $l=1$, respectively). We have used these potentials to calculate the self-consistent band structure of silicon and germanium, obtaining excellent agreement with photoemission data.[52]

We would like to emphasize that the experimental data pertaining to the electronic structure of atoms and solids plays a distinctly different role in the presently developed first-principles pseudopotentails than in the various empirical model potential approaches. This data is no longer used to fix the parametric form of the potential, but rather serves as a feedback in understanding the microscopic nature of the underlying electronic interactions. This permits a critical analysis of the many-body theory derived correlation functionals, and might hopefully lead to their systematic improvement in light of the available comparisons with experimental data.

VIII. SUMMARY

We have presented a method for obtaining a first-principles nonlocal atomic pseudopotential in the density-functional approach by directly inverting the exact pseudopotential eigenvalue problem. The resulting pseudopotentials yield the exact LDF ground-state eigenvalues valence spectra and wave functions which are unitarily rotated relative to the all-electron functions within maximum similarity and smoothness constraints. These pseudo potentials are only weakly energy dependent in an energy range of about a Rydberg, and hence yield very accurate wave functions, energy eigenvalues, and total energy differences over a wide range of excited configurations. We find that these potentials reproduce the chemical regularities of the Periodic Table, and that their characteristic features (classical turning points, radii of minimum potential, etc.) form nondigital coordinates which reflect the scattering power of the atomic cores by electrons in various angular-momentum states.

TABLE VI. Expansion coefficients of the pseudo-orbitals [Eq. (17)] for the $3d$ series. $\langle P_c\rangle_{nl}$ denotes the expectation value of the core-projection operator.

Element	Valence configuration	C_{1s}	C_{2s}	C_{3s}	C_{4s}	C_{2p}	C_{3p}	C_{4p}	$\langle P_c\rangle_{4s}$	$\langle P_c\rangle_{4p}$
Cr	$s^1p^0d^5$	−0.000 116 3	0.013 32	−0.2646	0.9643	0.004 436	−0.1545	0.9879	0.0702	0.0239
Mn	$s^2p^0d^5$	−0.000 131 0	0.014 87	−0.2833	0.9589	0.005 612	−0.1791	0.9838	0.0805	0.0321
Fe	$s^2p^0d^6$	−0.000 132 3	0.014 64	−0.2782	0.9604	0.005 357	−0.1708	0.9853	0.0776	0.0292
Co	$s^2p^0d^7$	−0.000 135 4	0.014 45	−0.2733	0.9618	0.005 121	−0.1628	0.9866	0.0749	0.0265
Ni	$s^2p^0d^8$	−0.000 135 7	0.014 18	−0.2684	0.9632	0.004 858	−0.1551	0.9879	0.0722	0.0241
Cu	$s^1p^0d^{10}$	−0.000 115 7	0.012 07	−0.2389	0.9709	0.003 215	−0.1106	0.9939	0.0522	0.0121
Zn	$s^2p^0d^{10}$	−0.000 133 8	0.018 60	−0.2593	0.9657	0.004 381	−0.1407	0.9900	0.0674	0.0198
Ga	$s^2p^1d^{10}$	−0.000 171 6	0.017 28	−0.3121	0.9499	0.008 177	−0.2359	0.9717	0.0977	0.0557
Ge	$s^2p^2d^{10}$	−0.000 176 1	0.017 93	−0.3153	0.9488	0.008 217	−0.2254	0.9742	0.0991	0.0508
As	$s^2p^3d^{10}$	−0.000 211 5	0.020 78	−0.3461	0.9379	0.010 96	−0.2765	0.9609	0.1202	0.0766
Se	$s^2p^4d^{10}$	−0.000 520 8	0.026 52	−0.3687	0.9292	0.012 93	−0.2967	0.9548	0.1367	0.0882
Br	$s^2p^5d^{10}$	−0.000 562 9	0.028 48	−0.3826	0.9234	0.014 44	−0.3131	0.9496	0.1471	0.0982

The nonempirical nature of these potentials permits systematic improvements in the underlying interaction model. As an example, we show how self-interaction and free-electron correlation corrections can be directly incorporated in the potentials, leading to improved results. These potentials are readily applicable to studies of molecular and solid-state electronic properties and phase stabilities, as they correctly represent both the low- and high-momentum components. In a subsequent paper we show how these potentials are used for studies of the electronic structure of bulk Si and Ge, and the transition metals Mo and W and for providing accurate phase separation of various octet and suboctet compounds.

ACKNOWLEDGMENTS

This work was supported in part by the Division of Basic Energy Sciences, U.S. Department of Energy and by NSF Grant No. DMR76-20647-A01.

APPENDIX A

To demonstrate the nature of the maximum similarity constraint of the pseudo-wave-function, we give, in Table VI, the wave-function expansion coefficients $C_{nl,n'l}$ [Eq. (12)] and the expectation value of the core projection operator $\langle\hat{P}_c\rangle_{nl}$ for the first transition series. The coefficients are given for the outermost valence s function $\chi_{4s}(r)$ as well as for the p function $\chi_{4p}(r)$:

$$\chi_{4s}(r) = C_{1s}\psi_{1s}(r) + C_{2s}\psi_{2s}(r) + C_{3s}\psi_{3s}(r) + C_{4s}\psi_{4s}(r); \tag{A1}$$

$$\chi_{4p}(r) = C_{2p}\psi_{2p}(r) + C_{3p}\psi_{3p}(r) + C_{4p}\psi_{4p}(r). \tag{A2}$$

As no core states of d symmetry occur in this series,

$$\chi_{3d}(r) = \psi_{3d}(r). \tag{A3}$$

All the results given are obtained from a Kohn and Shan atomic calculation with an exchange coefficient of $\alpha = \frac{2}{3}$. The departure of the $\langle P_c\rangle_{nl}$ values from zero [measuring the amount of core admixture in $\chi_{nl}(r)$] reflects the global similarity of the latter to the true wave function $\psi_{nl}(r)$: as $\langle P_c\rangle_{nl}$ decreases, the similarity is increased. These values of $\langle P_c\rangle_{nl}$ describe the least amount of core admixture into $\psi_{nl}(r)$ necessary to cancel all nodes in the latter and to obtain a low kinetic energy smooth pseudo-orbital with minimal amplitude in the core region (where the pseudopotential description of the electronic interaction is deficient). It is seen that even for the heaviest members of this series, the core admixture does not exceed 15% for the s wave functions and 10% for the p functions.

The values of the coefficients change with the configuration and with the fashion in which the electrons are partitioned into core and valence, as discussed in the text. These changes affect, however, the resultant pseudopotential [Eqs. (14), (15)] only to second order. Tables of these coefficients with a larger number of significant figures as well as values for other elements are available from the authors upon request. These can be used to conveniently construct the pseudopotential from Eqs. (14) and (15) once the solutions to the all-electron atomic problem are known.

[1]L. Szasz and G. McGinn, J. Chem. Phys. 47, 3495 (1967); A. O. E. Animalu and V. Heine, Philos. Mag. 12, 1249 (1965); P. Csavinszky and R. Hucek, Int. J. of Quant. Chem. Suppl. 8, 37 (1974); S. Topiol, J. W. Moskowitz, C. F. Melius, M. D. Newton, and J. Jafri, ERDA Research and Development Report, New York University C00-3077-105 (1976).
[2]J. C. Barthelat and Ph. Durand, Chem. Phys. Lett. 16, 63 (1972); A. Redondo, W. A. Goddard, and T. C. McGill, Phys. Rev. B 15, 5038 (1977); A. U. Hazi and S. A. Rice, J. Chem. Phys. 48, 495 (1968); M. A. Ratner, S. Topiol, and J. W. Moscowitz, Chem. Phys. 20, 1 (1976), K. M. Ho, M. L. Cohen, and M. Schlüter, Chem. Phys. Lett. 46, 608 (1977).
[3]M. L. Cohen and V. Heine, in *Solid State Physics*, edited by H. Ehrenreich, F. Seitz, and D. Turnbull (Academic, New York, 1970), Vol. 24, p. 38; D. Brust, in *Methods in Computational Physics*, edited by B. Alder, S. Fernbach, and M. Rotenberg (Academic, New York, 1968), Vol. 8, p. 33.
[4]W. A. Harrison, in *Pseudopotentials in the Theory of Metals*, (Benjamin, New York, 1966); J. C. Phillips, *Bonds and Bands in Semiconductors* (Academic, New York, 1973).
[5]J. A. Appelbaum and D. Hamann, Rev. Mod. Phys. 48, 479 (1976); M. Schlüter, J. R. Chelikowsky, S. G. Louie, and M. L. Cohen, Phys. Rev. B 12, 4200 (1975); J. R. Chelikowsky and M. L. Cohen, Phys. Rev. B 13, 826 (1976); J. R. Chelikowsky, M. Schlüter, S. G. Louie, and M. L. Cohen, Solid State Commun. 17, 1103 (1975); S. G. Louie, K. M. Ho, J. R. Chelikowsky, and M. L. Cohen, Phys. Rev. 15, 5627 (1977).
[6]S. G. Louie and M. L. Cohen, Phys. Rev. B 13, 2461 (1976); S. G. Louie, J. R. Chelikowsky, and M. L. Cohen, Phys. Rev. B 15, 2154 (1977); G. A. Baraff, J. A. Appelbaum, and D. R. Hamann, Phys. Rev. Lett. 38, 237 (1977); W. E. Pickett, S. G. Louie, and M. L. Cohen, Phys. Rev. 17, 815 (1978).
[7]D. Stroud and N. W. Ashcroft, J. Phys. F 1, 113 (1971); V. Heine and D. Weaire, in *Solid State Physics*, edited by H. Ehrenreich, F. Seitz, and D. Turnbull (Academic, New York, 1970), Vol. 24, p. 250.
[8]Reference 4 and R. M. Martin, Phys. Rev. 186, 871 (1969); H. Wendel and R. M. Martin, Phys. Rev. Lett. 40, 950 (1978).
[9]N. W. Ashcroft and D. Stroud, *Solid State Physics* (unpublished).
[10]P. B. Allen and M. L. Cohen, Phys. Rev. 187, 525 (1969).
[11]P. O. Löwdin, Phys. Rev. 139, A357 (1965).
[12]J. D. Weeks and S. A. Rice, J. Chem. Phys. 49, 2741 (1968).
[13]E. Hückel, Z. Phys. 60, 973 (1930); R. Hoffmann, J. Chem. Phys. 39, 1397 (1963).
[14]R. G. Parr, in *Quantum Theory of Molecular Electronic Structure*, (Benjamin, New York, 1963).
[15]J. A. Pople and D. Beveridge, *Approximate Molecular Orbital Theory* (McGraw-Hill, New York, 1970).
[16]F. Bloch, Z. Phys. 52, 555 (1978); J. C. Slater and G. F. Koster, Phys. Rev. 94, 1498 (1954).
[17]J. Hubbard, Proc. R. Soc. London Sec. A 276, 238 (1963).
[18]J. Kondo, in *Solid State Physics*, edited by H. Ehrenreich, F. Seitz, and D. Turnbull (Academic, New York, 1969), Vol. 23, p. 183.
[19]H. Hellmann, J. Chem. Phys. 3, 61 (1935).
[20]J. C. Phillips and L. Kleinman, Phys. Rev. 116, 287 (1959).
[21]M. H. Cohen and V. Heine, Phys. Rev. 122, 1821 (1961).
[22]R. N. Euwema and L. R. Kahn, J. Chem. Phys. 66, 306 (1977).
[23]L. R. Kahn, P. Baybutt, and D. G. Truhlar, J. Chem. Phys. 65, 3826 (1976).
[24]I. V. Abarenkov and V. Heine, Philos. Mag. 12, 529 (1965); V. Heine and I. V. Abarenkov, Philos. Mag. 9, 451 (1963).
[25]L. Szasz and G. McGinn, J. Chem. Phys. 45, 7898 (1966).
[26]W. Saslow, T. K. Bergstresser, and M. L. Cohen, Phys. Rev. Lett. 16, 354 (1966); M. L. Cohen and T. K. Bergstresser, Phys. Rev. 141, 789 (1966).
[27]J. R. Chelikowsky and M. L. Cohen, Phys. Rev. B 10, 5095 (1974); 14, 556 (1976); K. C. Pandey and J. C. Phillips, Phys. Rev. B 9, 1552 (1974).
[28]N. W. Ashcroft, Phys. Lett. 73, 48 (1966); N. W. Ashcroft and D. C. Langreth, Phys. Rev. 159, 500 (1967).
[29]G. Simons, J. Chem. Phys. 55, 756 (1971).
[30]J. D. Weeks, A. Hazi, and S. A. Rice, Adv. Chem. Phys. 16, 783 (1969).
[31]J. A. Appelbaum and D. R. Hamann, Phys. Rev. B 8, 1777 (1973).
[32](a) M. L. Cohen, M. Schlüter, J. R. Chelikowsky, and S. G. Louie, Phys. Rev. B 12, 5575 (1975); (b) S. G. Louie, M. Schlüter, J. R. Chelikowsky, and M. L. Cohen, Phys. Rev. B 13, 1654 (1976); (c) S. G. Louie, K. M. Ho, J. R. Chelikowsky, and M. L. Cohen, Phys. Rev. Lett. 37, 1789 (1976); (d) J. Ihm, S. G. Louie, and M. L. Cohen, Phys. Rev. B 17, 769 (1978).
[33]W. H. E. Schwarz, Theor. Chim. Acta 11, 307 (1968); 11, 377 (1968); J. C. Barthelat and P. Durand, Chem. Phys. Lett. 16, 63 (1972).
[34]V. Bonifacic and S. Huzinaga, J. Chem. Phys. 60, 2779 (1974); 62, 1507, 1509 (1975).
[35]C. S. Ewig and J. R. Van Wazer, J. Chem. Phys. 63, 4035 (1975).
[36]W. H. E. Schwartz, Theor. Chim. Acta 24, 29 (1972).
[37]Th. Starkloff and J. D. Joannopoulos, Phys. Rev. B 16, 5212 (1977).
[38]L. R. Kahn and W. A. Goddard, Chem. Phys. Lett. 2, 667 (1968); C. F. Melius, W. A. Goddard, and L. R. Kahn, J. Chem. Phys. 56, 3347 (1972); W. A. Goddard, Phys. Rev. 174, 659 (1968).
[39]K. F. Freed, Chem. Phys. Lett. 29, 143 (1974).
[40]A. Zunger, S. Topiol, and M. A. Ratner (unpublished).
[41]A. Zunger and M. A. Ratner, Chem. Phys. 30, 423 (1978); S. Topiol, A. Zunger, and M. A. Ratner, Chem. Phys. Lett. 49, 367 (1977).
[42]P. C. Hohenberg and W. Kohn, Phys. Rev. 136, 864 (1964); W. Kohn and L. Sham, Phys. Rev. 140, 1133 (1965).
[43]J. C. Slater, *Self-Consistent Field for Molecules and Solids* (McGraw-Hill, New York, 1974).
[44]K. S. Singwi, A. Sjolander, P. M. Tosi, and R. H. Land, Phys. Rev. B 1, 1044 (1970).
[45]A. R. Gupta and K. S. Singwi, Phys. Rev. B 15, 1801 (1977); M. Rasolt and D. J. W. Geldart, Phys. Rev. Lett. 35, 1234 (1975).
[46]C. Froese-Fischer, *The Hartree-Fock Method for Atoms* (Wiley, New York, 1977).
[47]G. Simons and A. N. Bloch, Phys. Rev. B 7, 2754 (1973), J. St. John and A. N. Bloch, Phys. Rev. Lett. 33, 1095 (1974).
[48]E. S. Machlin, T. P. Chow, and J. C. Phillips, Phys. Rev. Lett. 38, 1292 (1977).
[49]It is noted from Eqs. (19) and (21) that the Simons-Bloch (Ref. 47) empirical potential, which has been successfully employed for separation of various crystal structures (Refs. 47, 48), corresponds to the first leading

term in our potential $U_l(r) - Z_v/r$, where $U_l(r)$ is replaced by its limiting form Eq. (21). Our potential hence shares the feature of the occurrence of turning points with the Simons-Bloch potential. Note, however, that the slow decay of C_l/r^2, as compared to the much faster decay of $U_l(r)$, yields unphysically extended wave functions with the former potential, Ref. 47, and hence this potential is of limited use for electronic-structure calculations.

[50]A. Zunger and M. L. Cohen Phys. Rev. Lett. 41, 53 (1978).

[51]It is seen that all the alkali atoms are characterized by an approximately constant weak potential, while only the potential radii discriminate between them. This is the origin of the success of the empty core model potential (Ref. 18) ($W_l^{\min} \simeq 0$, while $r_l^{\min}$ is a variable) for these systems. For the divalent and three-valent atoms, on the other hand, this approximation fails as both the W_l and the r_l coordinates are required to specify the potential (Ref. 24).

[52]A. Zunger and M. L. Cohen, Phys. Rev. B (to be published).

[53]L. Szasz, J. Chem. Phys. 49, 679 (1968); G. Simons, Chem. Phys. Lett. 18, 315 (1973).

[54]We have performed similar tests on the semiempirical self-consistent model pseudopotentials (Ref. 32). The results for the Si potential [Ref. 32(a)] indicate that the 3s and 3p energy eigenvalues deviate by 0.50 and 0.35 eV, respectively, from the all-electron ground-state results, while for the singly ionized $3s^2\,3p^1$ configuration the deviations are 1.32 and 1.24 eV, respectively. The corresponding deviations in the first-principles potentials are (identically) zero for the ground state and 0.08 and 0.11 eV for the s and p states of the singly ionized configuration, respectively. Similar results are obtained for the Ge semiempirical potential [Ref. 32(d)]. The carbon nonlocal semiempirical potential [Ref. 32(d)] produces deviations of 0.67 and 1.45 eV for the ground-state 2s and 2p eigenvalues, respectively, 0.72 and 1.64 eV for the $2s^1 2p^3$ configuration, and 0.81 and 1.68 eV for the singly ionized $2s^1 2p^2$ configuration. In both these cases, the errors associated with the first-principles potentials are well below 0.1 eV. The total energy difference corresponding to this ionization process is 15.48 eV using the semiempirical potential, 13.71 eV with the first-principles potential, and 13.70 eV with the all-electron potential. These should be compared with the observed ionization energy of 11.26 eV and the calculated first-principles pseudopotential value with inclusion of correlation corrections (Ref. 44) of 11.12 eV. We conclude that the first-principles pseudopotentials constitute about an order of magnitude improvement in the description of the atomic and low-lying ionic states, relative to the semiempirical potentials.

[55]E. J. Baerends and P. Ros, Chem. Phys. 2, 52 (1973); H. Sambe and R. H. Felton, J. Chem. Phys. 62, 1122 (1975); F. W. Averill and D. E. Ellis, J. Chem. Phys. 59, 6412 (1973).

[56]O. Gunnarsson, J. Harris, and R. O. Jones, Phys. Rev. B 15, 3027 (1977); J. Chem. Phys. 67, 3970 (1977); J. Harris and R. O. Jones, J. Chem. Phys. 68, 1190 (1978).

[57]A. Zunger and A. J. Freeman, Phys. Rev. B 15, 4716, 5049; 16, 906 (1977); 17, 2030 (1978).

[58]A. Zunger and A. J. Freeman, Phys. Rev. B 17, 4850 (1978).

[59]A. Zunger and A. J. Freeman, Int. J. Quantum Chem. Suppl. 10, 383 (1976); 11, 539 (1977).

[60]J. F. Janek, V. L. Moruzzi, and A. R. Williams, Phys. Rev. B 12, 1757 (1975).

[61]A. Zunger and A. J. Freeman, Phys. Rev. B 16, 2901 (1977).

[62]L. Hedin and A. Johansson, J. Phys. B 2, 1336 (1969).

[63]L. J. Sham and W. Kohn, Phys. Rev. 144, 390 (1966).

[64]W. B. Fowler, Phys. Rev. 151, 657 (1966); R. S. Knox and F. Bassani, Phys. Rev. 124, 652 (1961); L. F. Mattheiss, Phys. Rev. 133, A1399 (1964).

[65]L. F. Mattheiss, Phys. Rev. 134, A970 (1964); I. Petroff and C. R. Viswanathan, Phys. Rev. B 4, 799 (1971).

[66]O. Gunnarsson and B. I. Lundqvist, Phys. Rev. B 13, 4274 (1976).

[67]K. Schwarz, Chem. Phys. 7, 100 (1975).

[68]C. E. Moore, "*Atomic Energy Levels*," Circular 1, 467 U. S. Department of Commerce, Natl. Bur. Stand.

[69]I. Lindgren, Int. J. Quant. Chem. Suppl. 5, 411 (1971).

[70]E. Clementi and C. Roetti, *Atomic Data and Nuclear Data Tables* (Academic, New York, 1974), Vol. 14.

[71]Our values differ somewhat from those of Ref. 69 due to the use of a correlation functional in the present work and possible differences in the degree of self-consistence convergence.

[72]B. Y. Tong and L. J. Sham, Phys. Rev. 144, 1 (1966).